HEAT TRANSFER PERFORMANCE AND PIPING STRATEGY STUDY FOR CHILLED WATER SYSTEMS AT LOW COOLING LOADS

A Thesis

by

NANXI LI

Submitted to the Office of Graduate Studies of
Texas A&M University
in partial fulfillment of the requirements for the degree of

MASTER OF SCIENCE

Chair of Committee,	David E. Claridge
Committee Members,	Charles H. Culp
	Michael B. Pate
Head of Department,	Jerald A. Caton

December 2012

Major Subject: Mechanical Engineering

Copyright 2012 Nanxi Li

ABSTRACT

The temperature differential of chilled water is an important factor used for evaluating the performance of a chilled water system. A low delta-T may increase the pumping energy consumption and increase the chiller energy consumption.

The system studied in this thesis is the chilled water system at the Dallas/Fort Worth International Airport (DFW Airport). This system has the problem of low delta-T under low cooling loads. When the chilled water flow is much lower than the design conditions at low cooling loads, it may lead to the laminar flow of the chilled water in the cooling coils. The main objective of this thesis is to explain the heat transfer performance of the cooling coils under low cooling loads.

The water side and air side heat transfer coefficients at different water and air flow rates are calculated. The coefficients are used to analyze the heat transfer performance of the cooling coils at conditions ranging from very low loads to design conditions. The effectiveness-number of transfer units (NTU) method is utilized to analyze the cooling coil performance under different flow conditions, which also helps to obtain the cooling coil chilled water temperature differential under full load and partial load conditions. When the water flow rate drops to 1ft/s, laminar flow occurs; this further decreases the heat transfer rate on the water side. However, the cooling coil effectiveness increases with the drop of water flow rate, which compensates for the influence of the heat transfer performance under laminar flow conditions. Consequently,

the delta-T in the cooling coil decreases in the transitional flow regime but increases in the laminar flow regime.

Results of this thesis show that the laminar flow for the chilled water at low flow rate is not the main cause of the low delta-T syndrome in the chilled water system. Possible causes for the piping strategy of the low delta-T syndrome existing in the chilled water system under low flow conditions are studied in this thesis: (1) use of two way control valves; and (2) improper tertiary pump piping strategy.

DEDICATION

To my family

ACKNOWLEDGEMENTS

I would like to express my gratitude to my advisor, David E. Claridge. I could not have finished this thesis without his guidance and support. His encouraging words and valuable suggestions gave me a lot of help when I met difficulties throughout the thesis work.

I would also like to thank my thesis committee: Dr. Charles H. Culp and Dr. Michael B. Pate for their encouragement and comments. Thanks to Joseph Martinez and Ahmet Ugursal, for their help with the communications with the DFW airport and the collection of data.

I must thank my family, especially to my parents and husband. Thank you for their love. Thanks also to my friends and lab mates in Energy System Laboratory (ESL): Lei Wang, Guanjing Lin, Xiaoli Li, Juan Zhao, Jing Ji, and the ones who left the lab now: Song Deng, Qiang Chen, Liang Ma and Zhiqin Zhang. Thanks for all your encouraging words and support during the last two years.

NOMENCLATURE

A_a	Air Side Area
ACFM	Actual Cubic Feet per Minute
AHU	Air Handling Unit
A_w	Water Side Area
CFM	Cubic Feet per Minute
CHW	Chilled Water
CHWST	Chilled water Supply Temperature
C_p	Specific Heat
CUP	Central Utility Plant
DB	Dry Bulb
DFW	Dallas/Fort Worth
D_i	Inside diameter of the tube, ft
EDB	Entering Dry Bulb
EFT	Entering Fluid Temperature
EWB	Entering Wet Bulb
FH	Fin Height
FH	Fin Height
FL	Fin Length
FL	Fin Length
FPI	Fins per Inch

FPS	Feet per Second
GPM	Gallons per Minute
h_a	Air Side Heat Transfer Coefficient
h_{ae}	Entering Air Enthalpy
h_{al}	Leaving Air Enthalpy
h_s	Saturated Air Enthalpy
HVAC	Heating, Ventilating, and Air Conditioning
h_w	Water Side Heat Transfer Coefficient
L	Length of the tube, ft
LDB	Leaving Dry Bulb
LFT	Leaving Fluid Temperature
LMED	Log Mean Enthalpy Difference
LMTD	Log Mean Temperature Difference
LWB	Leaving Wet Bulb
N	the Number of Fins per Inch
NTU	Number of Transfer Units
Nu_w	Water Side Nusselt Number
Pr_w	Water Prendtl Number
Q	Heat Transfer Rate
Re_a	Air Reynolds Number
Re_w	Water Reynolds Number
SCFM	Standard Cubic Feet per Minute

SDVAV	Single Duct Variable Air Volume
T_{ae}	Air Temperature Entering the Cooling Coil
T_{al}	Air Temperature Leaving the Cooling Coil
T_s	Saturated Air Temperature
T_{we}	Entering Water Temperature
T_{wl}	Leaving Water Temperature
U	Overall Heat Transfer Coefficient
VSD	Variable Speed Drive
w_{ae}	Entering Air Humidity Ratio
w_{al}	Leaving Air Humidity Ratio
WB	Wet Bulb
w_s	Saturated Air Humidity Ratio
X_l	Longitude Tube Pitch
X_t	Transverse Tube Pitch
ε	Cooling Coil Efficiency
μ_b	Water viscosity at the water bulk temperature
μ_w	Water fluid viscosity at the pipe wall temperature
δ_F	Fin Pitch

TABLE OF CONTENTS

Page

LIST OF FIGURES

Page

LIST OF TABLES

Page

1 INTRODUCTION

1.1 Background and problem statement

Energy costs play an important role in today's industrial, residential, and commercial settings. Consequently, energy use becomes a factor which cannot be ignored during the design and management of a project. Air conditioning accounts for 44% of energy used in the commercial sector; commercial use is about 18.2% of the total energy used (EIA, 2010). Air conditioning is becoming more widely used in commercial buildings.

The chilled water system is a very important component in large air conditioning systems. The cooling coils in a chilled water system play a significant role since their geometric factors, such as size, number of rows, fin spacing, and fin profile, contribute to the air side pressure drop and affect the sound power level of the fans. Improper operation of the cooling coils will affect the chilled water piping, pumping, and even the efficiency of the chillers. The common structure of a cooling coil is shown in Figure 1.1. The chilled water cools and dehumidifies the moist air that flows over the external surface of the tubes and fins. To maintain a higher rate of heat transfer, the air and water normally follow a cross-flow or counter-flow arrangement.

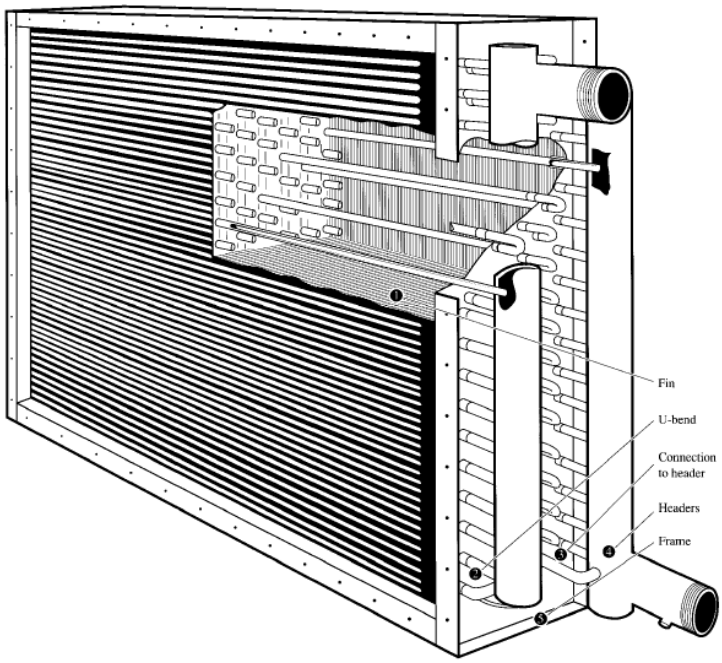

Figure 1.1 The structure of chilled water cooling coils (Wang, 1993, pp. 12.4)

To realize the reduction of energy use for a chilled water system, the chilled water cooling coil performance under different conditions should be considered. There are three kinds of flow types in the cooling coil tubes: laminar flow, transitional flow, and turbulent flow. The flow type is determined by the inside diameters of the tubes and the water flow velocity. The inside diameters of cooling coil tubes are related to the outside diameters and the tube-wall thickness. Common tube outside diameters are 5/16, 3/8, 1/2, 5/8, 3/4, and 1 inch. The tube wall thickness is mainly determined by the coil's working pressure and safety considerations.

Based on the hydraulic diameters of common cooling coils tubes, various ranges of water flow velocity in the tubes of cooling coils are recommended by different

standards and manufacturers. For nuclear HVAC applications, ASME Standard AG-1, Code on Nuclear Air and Gas Treatment, requires a minimum tube velocity of 2 fps. ARI Standard 410 requires a minimum of 1 fps or a Reynolds number larger than 3100. Most chilled water coils typically operate with tube-side water velocities in the range of 1 to 8 fps in conventional cooling systems that are operating at full load. Most coil manufacturer's software, which is used to select chilled water coils and predict coil performance, has the limitation that it can only predict coil performance when the water velocity is larger than 2 fps and the water flow is turbulent. However, under partial load conditions, tube-side water velocities can be less than 1 fps, which causes laminar flow in the tubes.

The cooling coils studied in this thesis are the coils planned for use in the DFW Airport, which are typically air-cooled plain-fin, and tube cooling coils manufactured by Temtrol. The data sheet for the design condition of the coils is shown in Table 1.1.

Table 1.1 Design condition for the cooling coil (Neal, 2011)

(Model number: 5WC-12-36×88×8-11 AL)

Total face area / Face velocity	44 ft^2 / 477.3 cfm
Coil FH×FL	36 inch×88 inch
Rows – FPI	8 – 11
Fin thickness / Material	0.008 inch / AL
Tube outside diameter / Wall	5/8 inch / 0.025 inch
ACFM / SCFM	21,000 / 19,722 cfm
EDB / EWB	82 / 68 ˚F
LDB / LWB	48.5 / 48.5 ^{O}F
Total heat / Sensible Heat	1,151,872 / 727,822 Btu/hr
LFT / EFT	38 / 61.9 ^{O}F
Water flow rate / velocity	96 GPM / 3.44 ft/s

To improve the performance of the chilled water system, the Energy Systems Laboratory (ESL) team analyzed the energy consumption of various pumps for operation alternatives at the central utility plant (CUP) of the DFW Airport (ESL, 2011). Based on the existing trend data for the major airport terminals and buildings provided by the engineering design teams, a central loop with tertiary pumping is the most viable option for operating the chilled water distribution loop with the expectation of future expansions. As a result, tertiary pumps are being considered for installation in the terminals in the DFW Airport to save annual chilled water system pumping energy use.

The ESL team also proposed a new tertiary pump schematic with potential locations for future valves and control components for the DFW Airport, as shown in Figure 1.2.

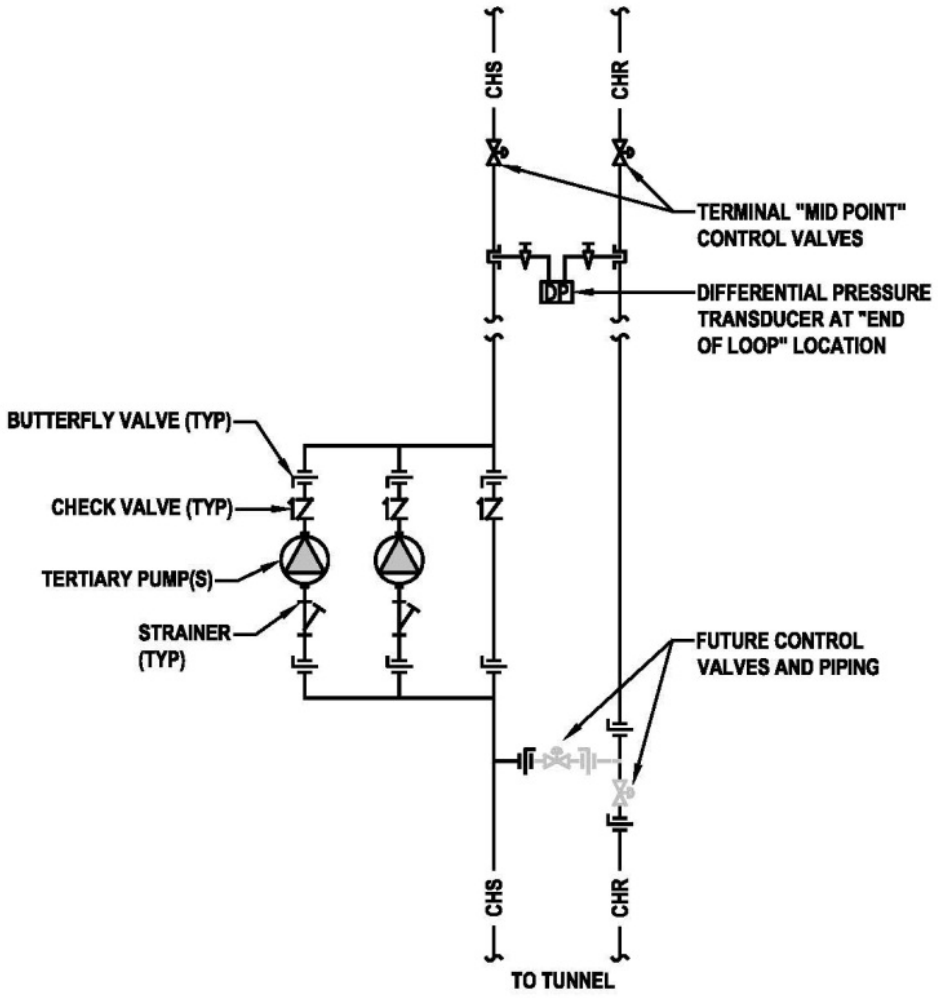

Figure 1.2 Proposed tertiary pump installation schematic (ESL, 2011)

The cooling loads of the terminals are influenced by several factors, such as the outside air temperature, humidity, the envelope characteristics, the number of occupants in the terminals, the operation of equipment, and lights. When the loads are low, the

tertiary loop pumps operate at low speed. Many chilled water valves are mostly closed because of the low cooling load requirement. Consequently, the cooling coils operate with low water flow rates. When the water flow velocity is lower than 1 fps, laminar flow occurs in the tubes. Low water flow velocity may also cause low delta-T syndrome in the cooling coils.

The low delta-T syndrome is the case when the temperature differential between the chilled water supply and the return water is low. This situation will increase the pump power consumption and negatively affect energy savings in the chilled water system. As a result, the heat transfer performance of the cooling coils under partial flow, especially for the laminar flow condition, should be studied to help analyze the cooling coil influence on the chilled water system delta-T performance.

Based on the 2010 chilled water system measured data in the DFW Airport, the temperature difference between supply and return chilled water temperatures dropped to a low of 50% of the design delta-T under low load conditions. The influence of laminar flow in the cooling coil for the chilled water system loop delta-T will be studied, and other possible causes for the chilled water system low delta-T syndrome in the system will also be analyzed.

1.2 Objective

The objective of the study is to investigate the causes of low delta-T at low loads in the DFW Airport chilled water loop. The investigation will initially analyze the heat transfer performance of cooling coils when the water flow switches from turbulent to transitional and then to laminar flow. A major goal is to determine the specific influence

of coil performance across a range of part-load conditions and water flow rates on the distribution loop delta-T. Other possible causes under low loads that will be investigated include the improper use of valves and high leaving air temperature for the low delta-T syndrome in the system. This study will fulfill this objective in three steps:

(1) The physical parameters and other cooling coil specifications, which include inside and outside area of the tubes, longitudinal fin pitch, and transverse fin pitch, are calculated based on the design conditions provided by the manufacturer. They will be utilized when analyzing of the cooling coils under the other operating conditions.

(2) The water side and air side heat transfer coefficients under different water and air flow rates will be calculated and used to analyze the heat transfer performance of the cooling coils under conditions ranging from very low loads to design conditions. The effectiveness-NTU method is utilized to analyze the cooling coil effectiveness under dry and wet conditions. The cooling coil chilled water temperature differential will then be obtained under full load and partial load conditions.

(3) The influence of the cooling coils on the chilled water loop delta-T performance will be analyzed. Results of the analysis will be compared with the weather data and chilled water system data of the DFW Airport during 2010. Other possible causes of the reduced delta-T at low loads exist and will be investigated.

2 LITERATURE REVIEW

2.1 Heat transfer performance influence factors

Chilled water cooling coils are often fin and tube heat exchangers, which consist of rows of tubes that pass through sheets of formed fins. The common outside diameters of the tubes are 5/16, 3/8, 1/2, 5/8, 3/4, and 1 inch, with fins spaced 4 to 18 per inch. Tube spacing ranges from 0.6 to 3.0 inch (ASHRAE, 2004). As the air passes through the coil and contacts the cold fin surfaces, heat transfers from the air to the chilled water flowing through the tubes. Fin and tube heat exchangers are widely used in the field of thermal engineering. While there are many fin patterns, such as plate, louver, convex-louver, and wavy, the plate-fin is the most popular pattern used in heat exchangers and cooling coil applications (Erek et al., 2005). The plate fin configuration has the advantages of simplicity, rigidity, and economic impact. The factors which may influence the heat transfer performance of the heat exchangers or cooling coils include the arrangement of the circuit configuration specification of fins and tubes, and operating conditions (Liu et al., 2004).

The fluid flow arrangement in coil tubes has a great influence on the performance of the heat transfer surface. Generally, cooling coils are multi-row and circuited for a combination of counter-flow and cross-flow arrangement. Counter-flow can produce the highest possible heat exchange, because it has the closest temperature relationships between the tube fluid and air at each side of the coil (ASHRAE, 2004).

Typical tube geometries used in heat exchangers include elliptical and circular. Webb (1980) verified through experiments that elliptical tubes have better heat transfer performance than circular tubes when all other conditions are the same.

Rich (1973) presented the effect of fin spacing on the heat transfer performance of multi-row, smooth plate fin, and tube heat exchangers. His experiments were based on a nine row heat exchanger with fin spacing within the range of 3 to 21 fins per inch. The results showed that the heat transfer coefficient is independent of the fin spacing when the other parameters are kept constant; however, the air side thermal resistance is decreased when the fin spacing is reduced. Romero-Mendez et al. (2000) utilized flow visualization and numerical computation techniques to determine the effect of the distance of two fins on the total heat transfer rate for a single row fin and tube heat exchanger. This research demonstrated that the fin spacing will strongly influence the overall Nusselt number and the pressure drop in the heat exchanger. Many of the conclusions can also be applied to multi-row devices.

Wang and Chi (2000) further reported the influence of tube rows, fin pitch, and tube diameter on heat transfer and pressure drop of a plate fin and tube exchanger. They concluded that when the number of tube rows is increased from 2 to 4 with the tube diameter at 8.51 mm and the fin pitch at 2.06 mm, the heat transfer coefficient decreased as much as 60% when the Reynolds number is less than 3,000. The drop of heat transfer coefficient is less than 15% for the condition when the Reynolds number is larger than 10,000. Moreover, for the same experimental conditions with fin pitch at about 1.23 mm,

the difference for the heat transfer coefficients of coils with different tube diameters, 8.51 mm and 10.23 mm, is less than 10%.

Following previous researchers, this thesis will focus on the heat transfer performance of cooling coils in the DFW Airport. The cooling coils studied are plate fin type with 8 rows of circular tubes and 11 fins per inch. The fluid flow is a combination of cross-flow and counter-flow. However, it will be simplified as cross-flow, since the cross-flow is the major pattern in the coils. Further information about the cooling coils can be found in Table 1.1.

2.2 Modeling of heat exchangers performance

2.2.1 Different modeling methods

The most widely used method to model the heat exchangers performance is the Log Mean Temperaure Difference (LMTD) method.

Based on the assumption that overall heat transfer coefficient U for the total external surface is constant, Mueller (1973) proposed the log mean temperature method for the analysis of heat exchanger performance under dry conditions:

$$Q = UAF\Delta T_{lmtd} \tag{2.1}$$

Where A is the coil face area, F is the correction factor, ΔT_{lmtd} is defined as the log mean temperature difference, and Q is the cooling load.

$$\Delta T_{lmtd} = \frac{(T_{ae} - T_{wl}) - (T_{al} - T_{we})}{\ln\left[\frac{(T_{ae} - T_{wl})}{T_{al} - T_{we}}\right]} \tag{2.2}$$

U for a heat exchanger can be calculated from:

$$\frac{1}{UA_a} = \frac{1}{\eta h_a A_a} + \frac{dx_t}{kA_t} + \frac{1}{h_w A_w} \quad \textbf{(2.3)}$$

η is the efficiency of the air side surface, k is the thermal conductivity of the tube wall. The thermal resistance of the tube wall is almost always negligible, so the overall heat transfer coefficient for the heat exchanger can be simplified to:

$$\frac{1}{UA_a} = \frac{1}{\eta h_a A_a} + \frac{1}{h_w A_w} \quad \textbf{(2.4)}$$

For the cooling coils when wet, the Log Mean Enthalpy Difference (LMED) method should be utilized for the heat transfer estimation between the air and the surface of the tubes. The LMTD method will be used to evaluate the heat transfer between the water and the surface. The LMED method considers the latent heat transferred by replacing the temperatures of the entering/leaving air/water with their respective enthalpies. Finally, when the cooling coils are partially wet, the boundary between the dry and wet surfaces needs to be calculated by an iterative process; then the dry and wet parts of the coil need to be considered separately. The summary for the analysis of cooling coils under different situations is presented in the ASHRAE Systems and Equipment Handbook (2004). However, this method was not used in this thesis because it requires extensive details of the physical characteristics of the cooling coil and it also includes an extensive calculation and iteration process.

Researchers have also investigated some other strategies for modeling heat exchangers. Zhao (1995) analyzed the performance of a single-row heat exchanger at low in-tube water flow rates by a neural network method and developed a theoretical

model to simulate the dynamic heat transfer process for a single-row heat exchanger. The disadvantages of this method are that it is limited to the single-row heat exchanger .

Khan et al. (2006) developed analytical models for heat transfer in cross-flow heat exchangers with a bank of tubes, for both in-line and staggered arrangements. The models are developed in terms of transverse pitch, longitudinal pitch, Reynolds number, and Prandtl number. These four parameters all contributed to the average heat transfer coefficient. Moreover, the staggered arrangement results in higher heat transfer rates than the in-line arrangement.

Wang et al. (2004) proposed a simplified hybrid model of cooling coils for control and optimization of HVAC systems. The model, with no more than three characteristic parameters, captures the inherent nonlinear characteristics of a cooling coil unit (CCU) compared with the other linear models. However, this model requires the pressure difference across the CCU, which is not available in this case.

Braun (1989) proposed the effectiveness-NTU method for modeling cooling towers and cooling coils. Effectiveness relationships are developed through the introduction of an air saturation specific heat. These relationships can be used to set up heat transfer models for cooling coils under dry, wet, and partially wet conditions. Moreover, for the partially wet conditions, Braun assumed the cooling coils were initially completely dry or wet to get two results; then he chose the larger value as the result of partially wet conditions. He proved that the error of this method when used to estimate the heat transfer of cooling coils under partially wet conditions is less than 5%.

Considering these advantages, the effectiveness-NTU method is used to analyze the heat transfer between the chilled water and air in this thesis.

2.2.2 Water side heat transfer

The heat transfer coefficient and the Nusselt number of the water side in cooling coils are related to the Reynolds number and the Pandtl number of the water. The following correlations to estimate the water side heat transfer coefficient in the cooling coils are recommended for single-phase convective flow in the pipe flow. Since the water flow condition can be divided into laminar flow, transitional flow, and turbulent flow, different correlations may only be applied to a specific range of Reynolds numbers.

The Dittus-Boelter (1930) correlation is recommended by the industry standard (ARI, 1987) for the calculation of water side heat transfer with Re_w >10,000. As a result, it is usually used for fully developed turbulent flow inside smooth and round tubes.

The Gnielinski (1976) correlation can be used for transitional flow and turbulent flow conditions when the Reynolds number satisfies: 3,000 < Re_w < 5×10^6.

Petukhov (1970) correlation has a higher requirement for the Reynolds number of the water in the pipes, and it is used for $10^4 < Re_w < 5 \times 10^6$. Similar to the Gnielinski correlation, it also introduces f_w to help with the final calculation.

The Sieder-Tate (1936) correlation has the advantage that it takes into account the change in viscosity due to temperature change between the bulk fluid average temperature and the heat transfer surface temperature.

Mirth and Remadhyani (1993) presented an experimental setup to obtain heat transfer and pressure drop data from commercially available chilled water cooling coils.

The deviations between the experimental results and the manufacturers' performance predictions for the cooling coils are pointed out. The authors recommended that the Gnielinski correlation should be used to predict the water side heat transfer coefficient for cooling coils operating at water side Reynolds numbers exceeding 2300.

2.2.3 Air side heat transfer

The fin surface of the cooling coils may be fully wet, fully dry, or partially wet depending on the difference between the dew point temperature of the entering and surface temperature. The dry or wet condition of the heat exchanger surface may influence the heat transfer coefficient on the air side, since the condensate retained on the surface of a heat exchanger may have hydrodynamic effects by changing the surface geometry and the air flow pattern. A water layer on the surface increases local surface heat transfer resistance (Abdenour et al., 2011).

McQuiston (1978) proposed the first general correlation of air side heat transfer coefficient for the heat exchanger with plain fin, which is the most widely used fin pattern for fin and tube heat exchangers. This correlation is based on the test results of five test samples.

Chen et al. (1995) developed an air side correlation for plain fin and tube heat exchangers in wet conditions. The correlations used 31-fin and tube heat exchangers as the samples. The proposed heat transfer correlation can describe 93.4% of the test data within $\pm$15% with a mean deviation of 6.33%.

The most common method used to calculate the air side heat transfer coefficient in heat exchangers was proposed by Wang et al. in 1997, in which he analyzed the air

side performance of plain-finned tube heat exchangers under dehumidifying conditions. Wang et al. (2000) also proposed a method to calculate the air side heat transfer coefficient of plain finned tube heat exchangers under dry surface conditions. This method is used in this thesis to calculate the air side heat transfer coefficient.

2.3 The low delta-T syndrome in the chilled water system

The low delta-T syndrome occurs when the temperature differential between the chilled water supply and return water temperature is low. When the low delta-T syndrome happens, a series of operation problems will occur, such as an inability to operate the chillers with sufficient load, excess water flow demand, increase in pump energy, and either an increase in chiller energy or failure to meet cooling coil demand. Therefore, the low delta-T syndrome in a chilled water system is a problem that should be avoided or mitigated (Ma et al., 2010).

Taylor (2011) studied the typical annual energy use versus chilled water delta-T with a constant chilled water supply temperature and constant pipe sizes. Although the fan energy consumption increases slightly as the chilled water delta-T increases, the reduction of chilled water pump and chiller energy consumption leads to the decrease of overall energy consumption of about 10% when delta-T increases from 11 ºF to 20 ºF.

Due to the detrimental influence of the delta-T syndrome on the operation of the chilled water system, the causes of low delta-T are studied by many researchers. Taylor (2002) addressed the causes of degrading delta-T along with mitigation measures. The causes of low delta-T syndrome are broken into three categories in this paper: causes that can be avoided, causes that can be resolved but may not result in energy savings,

and causes that cannot be avoided. The laminar flow in the cooling coil is introduced in the second category.

Wang et al. (2006) studied the factors, such as cooling coil size, chilled water supply temperature, outside air flow, space cooling load, coil fouling condition, and so on, which may cause low delta-T syndrome in a district cooling system. The influences for the delta-T of these factors are compared in the simulation with the conclusion that the main cause for the low delta-T syndrome for the system in the simulation is the improper use of 3-way control valves.

Kirsner (1996) pointed out that the low delta-T can be caused by dirty cooling coils, throttling valves with insufficient shutoff capability, reset CHS temperature, and poorly controlled blending station. Kirsner (1998) also analyzed the demise of the standard primary-secondary chilled water system: it cannot respond to the low delta-T syndrome due to the constant flow through the primary loop.

Many strategies have been proposed to solve or mitigate the low delta-T syndrome in the chilled water system. Florino (1999) recommended several practical methods to achieve high chilled water delta-T in variable flow cooling systems, which will reduce the pressure losses and pumping energy in existing systems. The methods ranged from the detailed component of the system to the distribution system configurations.

Severini (2004) described the philosophy for the design and operation of primary-secondary chilled water systems, which use a bypass check valve to optimize the chilled water delta-T.

Taylor (2002) categorized and summarized the possible solutions for low delta-T syndrome existing in the chilled water system. These solutions include valve selection, coil selection, control strategies for the chilled water supply temperature, and supply air temperature.

Hartman (2001) brought up three methods to deal with the low delta-T syndrome, which include installing pumps in series, deleting the decouple line, and paying close attention to the delta-T in each loop.

2.4 Cooling coil performance under different water flow conditions

Above certain water flow rates, turbulent flow happens in the cooling coils and makes water splash against the inside wall of tubes. It is helpful in the heat transfer efficiency of cooling coils and most testing is based on this condition. On the other hand, when the velocity of water through the coils becomes too small, usually below 1 fps, the water flow in the tubes will be in a laminar flow condition. When laminar flow happens, some of the water gets caught in the center of the tube and never comes into contact with the tube wall. This condition generally causes great unpredictability in coil performance (USA Coil and Air News Letter, 2012).

Some studies (Nonnenmann, 2012) claimed that the low delta-T syndrome will be caused when the water flow rate is relatively low in the tubes of the cooling coils. When water flow in a cooling coil becomes laminar, the heat transfer coefficient between the water and the inside of the tube suddenly falls, and it will reduce the capacity of the coil and cause low delta-T syndrome (Montgomery, 2009). Keeping the water flow at turbulent flow regime is important for maintaining the cooling coil to work

properly.

There are two ways recommended to reduce or avoid the negative heat transfer influence of laminar flow in the cooling coils (Green Building HVAC, 2012): (1) Special spirals are sometimes offered by manufacturers to enhance coil heat transfer efficiency and avoid a low delta-T. These are installed inside tubes and help to maintain turbulent water flow inside tubes. (2) Small terminal circulators are used to maintain desirable velocity inside tubes. These are small pumps which are selected according to the pressure drop of the cooling coil. They keep water moving at all operating points.

Contrary to the studies identified above, additional researchers suggest an opposite opinion regarding the influence of cooling coil performance under low cooling loads for the low delta-T syndrome in the chilled water system.

Landman (1991) used the ARI-certified Trane cooling coil performance program to simulate the coil performance. The program shows that the leaving water temperatures under a half-load condition in variable air volume (VAV) and constant air volume (CAV) systems are both higher than the full-load condition.

Taylor (2002) used a coil manufacturer's expanded simulation program and proved that although chilled water delta-T in cooling coils begins to fall as a function of coil tube velocity under partial load conditions, the delta-T below the onset of laminar flow increases rather than decreases.

However, the cooling coil performance at part-load conditions in these studies were performed using commercial software that is not available to the public. Consequently, the results are limited to the cooling coil model provided by the

manufacturer. This thesis will study the performance of cooling coils in the DFW Airport based on the effectiveness-NTU model so that it can provide evidence about the role of cooling coil performance under the different load conditions in the chilled water system.

3 METHODOLOGY

The study of heat transfer performance and piping strategy for the chilled water system under low cooling loads is based on the chilled water system and cooling coils in the DFW Airport. The first stage is to develop the cooling coil model utilizing the effectiveness-NTU model. To complete the model, the overall heat transfer coefficient obtained from water side and air side heat transfer coefficients will be studied. The system variables in the model include the entering water temperature, leaving water temperature, water flow rate, entering air temperature, leaving air temperature, and air flow velocity.

3.1 Model development

As shown in Table 3.1, the design condition of the cooling coil is provided by the manufacturer of the cooling coils that are in the DFW Airport. The other physical parameters, which are used for the following model development, such as the tube inside area (A_i), tube outside area (A_o), transverse tube pitch, and longitudinal tube pitch are estimated and calculated based on the manufacturer's data sheet (see Table 3.1). The following assumptions for the Air Handling Unit (AHU) with the coils that are used in the model are based on the control strategy of the chilled water system in the DFW Airport: (1) The AHU is a Single Duct Variable Air Volume (SDVAV) system. Figure 3.1 shows the schematic of the system. (2) The leaving air temperature is 55 ºF. (3) The minimum outside air ratio is 20%.

Table 3.1 Simulation baseline

Total face area / Face velocity	44 ft2 / 477.3 cfm
Coil FH×FL	36 inch×88 inch
Rows – FPI	8 – 11
Fin thickness / Material	0.008 inch / AL
Tube outside diameter / Wall	5/8 inch / 0.025 inch
Interior tube wall area Ai	759 ft2
Exterior tube wall area Ao	9995 ft2
Transverse tube pitch	0.15ft
Longitudinal tube pitch	0.068ft
EDB / EWB	82 / 68 ˚F
LDB / LWB	55 / 55 ˚F
LFT / EFT	38 / 62 ˚F
Design water flow rate / velocity	83 GPM / 2.97 ft/s
Design air volume flow rate	21,000 cfm
Minimum air volume flow rate	4,200 cfm (20% of the design value)

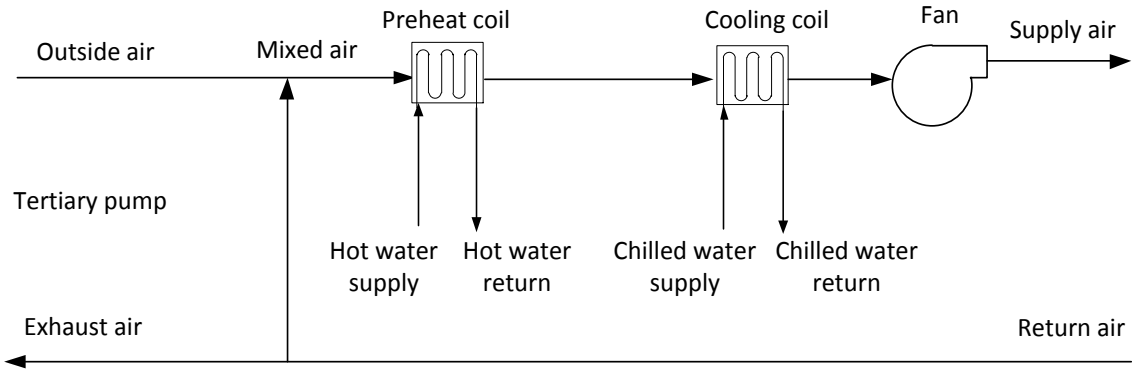

Figure 3.1 Configuration of an SDVAV system

With the water and air flowing through the system, the temperatures of the water and the air decrease, so their properties will also change during this process. The change of their properties can be considered by the finite element method (Wang et al., 2005). However, the model in this thesis is based on some assumptions to simplify the problem. The assumptions the influence of these assumptions are as follows:

(1) The chilled water in the cooling coils is incompressible, which assumes that the density of the chilled water in the cooling coil is constant, and the velocity of the water is uniform. The increase of the water velocity and density will cause the increase of the water Reynolds number and the water side heat transfer coefficient.

(2) The mixture for air and water vapor is an ideal gas and the air velocity is uniform when it goes through the tubes. The increase of air velocity will also increase the air Reynolds number.

(3) The densities and specific heats of air and water are constant and are based on the values of air and water at the average temperatures in the coil.

3.2 Water side heat transfer

3.2.1 Water side heat transfer coefficient models under turbulent flow

There are four correlations commonly used to calculate the water side heat transfer coefficient for cooling coils when the water flow is turbulent in the tubes.

a) The Dittus-Boelter (1930) correlation

The Dittus-Boelter correlation is recommended by the industry standard (ARI, 1987) for the calculation of water side heat transfer with $Re_w \geq 10000$, $0.6 \leq Pr_w \leq 160$, $L/D \geq 10$:

$$Nu_w = 0.023 Re^{0.8} Pr^{0.4} \tag{3.1}$$

b) The Gnielinski (1976) correlation

The Gnielinski correlation is used for turbulent flow for $3{,}000 < Re_w < 5 \times 10^6$, $0.5 < Pr_w < 2000$:

$$Nu_w = \frac{\left(\frac{f_w}{8}\right)(Re_w - 1000)Pr_w}{1.07 + 12.7\left(\frac{f_w}{8}\right)^{\frac{1}{2}}\left(Pr_w^{\frac{2}{3}} - 1\right)} \tag{3.2}$$

$$f_w = (0.79 ln Re_w - 1.64)^{-2} \tag{3.3}$$

c) The Petukhov (1970) correlation

The Petukhov correlation has a higher requirement for the Reynolds number of the water in the pipes, and it is used for $10^4 < Re_w < 5 \times 10^6$:

$$Nu_w = \frac{(\frac{f_w}{8})Re_w Pr_w}{1.07 + 12.7(\frac{f_w}{8})^{\frac{1}{2}}(Pr_w^{\frac{2}{3}} - 1)}(\frac{\mu_b}{\mu_s})^{0.25} \quad \textbf{(3.4)}$$

d) The Sieder-Tate (1936) correlation

The Sieder-Tate correlation has the advantage that it takes into account the change in viscosity due to temperature change between the bulk fluid average temperature and the heat transfer surface temperature. For turbulent flow, $Re_w \geq 10000$, $0.6 \leq Pr_w \leq 16700$, $L/D \geq 10$:

$$Nu_w = 0.027Re^{0.8}Pr^{\frac{1}{3}}(\frac{\mu_b}{\mu_w})^{0.14} \quad \textbf{(3.5)}$$

μ_b — Water viscosity at the water bulk temperature

μ_w — Water fluid viscosity at the pipe wall temperature

D_i — Inside diameter of the tube, ft

L — Length of the tube, ft

Figure 3.2 shows the relationship between different correlations for the water under turbulent flow with an average temperature of 50ºF in the tubes. The Petukhov correlation has the highest values, while the Sieder-Tate correlation has the lowest in the turbulent flow regime. The range of Gnielinski correlation is wide; the Reynolds number can start from 3000, and it is recommended by Mirth and Remadhyani (1993) since it gets closer results in their study using an experimental setup. The value of Gnielinski correlation is between the Petukhov and Sieder-Tate correlations for most turbulent flow conditions. In this thesis, for the turbulent flow of water in the cooling coils, the

Gnielinski correlation will be used to analyze the heat transfer performance when the Reynolds number is larger than 3,000.

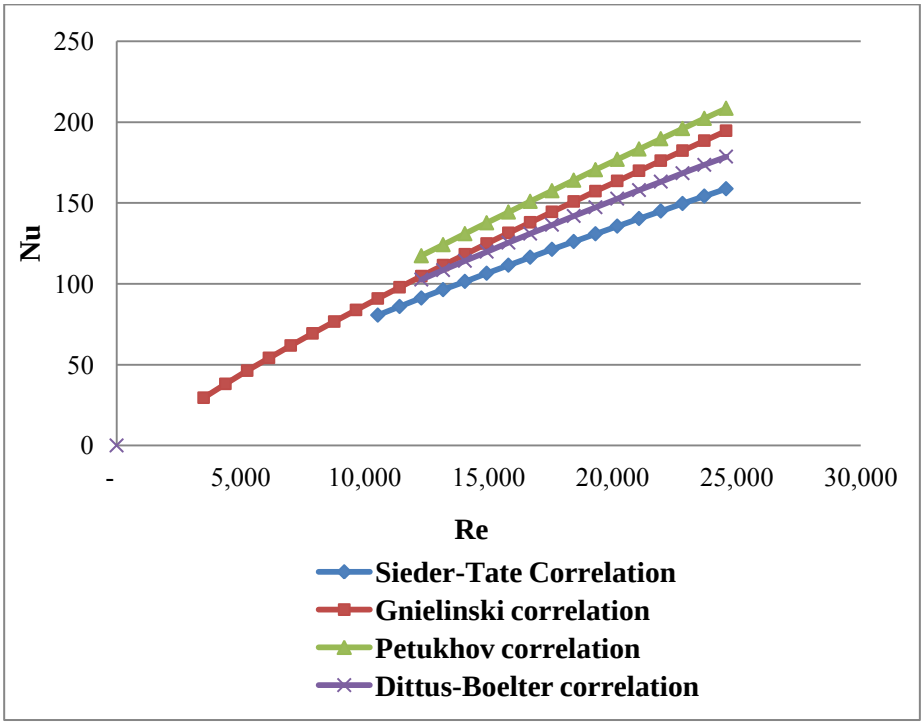

Figure 3.2 Water Nusselt number for turbulent flow under different water side heat transfer correlations

3.2.2 Water side heat transfer coefficient models under laminar flow

For the conditions where the Reynolds number of the water flow is less than2,300, it enters the laminar flow regime.

The Sieder –Tate correlation is proposed to calculate the Nusselt number for the short tubes:

$$Nu_w = 1.86 Re^{\frac{1}{3}} Pr^{\frac{1}{3}} \left(\frac{D_i}{L}\right)^{\frac{1}{3}} \left(\frac{\mu_b}{\mu_w}\right)^{0.14} \quad \textbf{(3.6)}$$

Incropera and DeWitt proposed that the Nusselt number for the long tubes in the cooling coils under laminar flow is constant: (1) $\mathrm{Nu_w} = 4.36$ for the uniform surface heat flux; and (2) $Nu_w = 3.36$ for uniform surface temperature.

3.2.3 Water side heat transfer performance

The models used in this simulation are the Gielinski correlation for the turbulent flow conditions. The water Reynolds number and water side heat transfer coefficient follow linear relationship in this range. For the laminar flow conditions, since the cooling coil tubes is long ($L/D \geq 10$), the Sieder-Tate correlation is not recommended in this case. Moreover, for the long tubes with several rows, the surface temperature different cannot be neglected. If the heat flux is assumed to be constant in the laminar flow, the Nusselt number is 4.36 for the conditions when $0 < Re_w < 2{,}300$. Since the heat transfer in the transitional flow condition is difficult to predict, no correlation provides an accurate relationship between the Reynolds number and the heat transfer coefficient of water. Linear interpolation is assumed in the transitional regions between the turbulent and laminar regions. As shown in Figure 3.3, when the water flow rate and viscosity are constant, the water Reynolds number is proportional to the flow rate in the turbulent conditions. The water heat transfer coefficient decreases significantly when the flow becomes transitional and laminar ($Re_w < 3000$). The entering water temperature is 38 ˚F and the leaving water temperature is 62 ˚F , so the average water temperature in the cooling coil is 50˚F ,

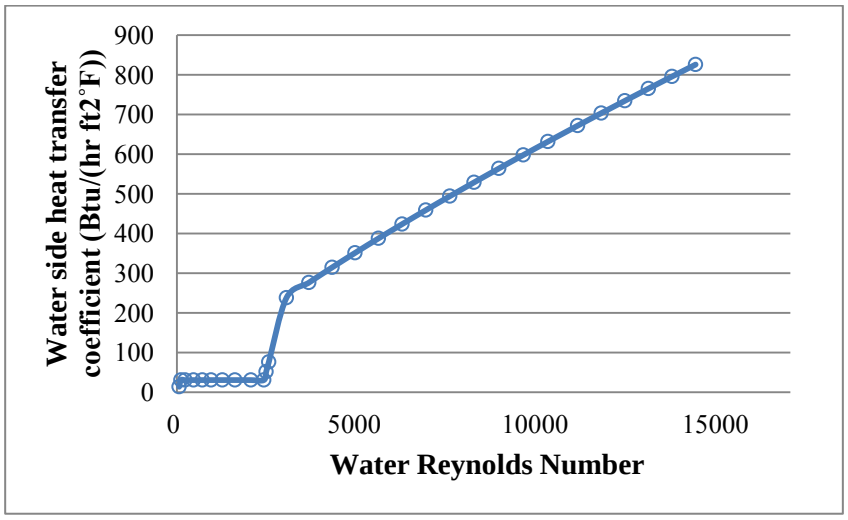

Figure 3.3 Water side heat transfer coefficient vs. water Reynolds number

If the Nusselt Number (Nu) of water can be obtained from the above correlations; and the inside diameter (Di) of the tube is known; and the specific heat of water (k) is determined by the average temperature of the water; then, the water side heat transfer coefficient (h) can be calculated from:

$$h = \frac{Nu \times k}{D_i} \quad \textbf{(3.7)}$$

. The water flow becomes transitional flow and then laminar flow when the water flow velocity is lower than 1 ft/s. The water heat transfer coefficient not only decreases as the water flow velocity decreases, but also significantly drops when the water velocity is lower than 1 ft/s (see Figure 3.4).

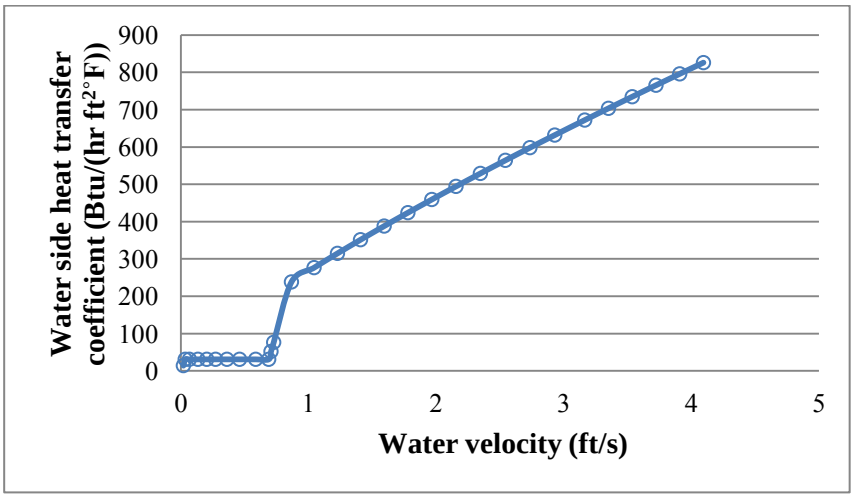

Figure 3.4 Water side heat transfer coefficient vs. water velocity

3.3 Air side heat transfer

3.3.1 The air volume flow rate and cooling load

There are two types of cooling load: sensible cooling load and latent cooling load. When the load in the buildings is changed, the volume of supply air will be adjusted in order to maintain the indoor temperature, so the cooling load of the cooling coils will also change (Coad, 1998). The calculations of the two types of cooling load are as follows:

1) Sensible cooling load

The amount of heat transferred from the air can be expressed as following:

$$Q_{sensible} = \rho \times \dot{V} \times C_p \times \Delta T \quad \textbf{(3.9)}$$

ρ = the density of the air (lb/ft^3)

$\dot{V}$= the volume flow rate of the air (ft^3/min)

C_p= Specific heat of the air (Btu/lb-°F)

ΔT = the change in dry bulb temperature of the air (°F)

$$Q_{sensible} = 1.08 \times \dot{V} \times \Delta T \quad \textbf{(3.10)}$$

2) Latent cooling load

The latent cooling load can be obtained from the difference between the total cooling load and sensible cooling load:

$$Q_{latent} = Q_{total} - Q_{sensible} \quad \textbf{(3.11)}$$

The equation for calculating the total heat added to the water from the air is:

$$Q_{total} = \rho \times \dot{V} \times \Delta h \quad \textbf{(3.12)}$$

Δh = the change for the enthalpy of the air (Btu/)

$$Q_{total} = 4.5 \times \dot{V} \times \Delta h \quad \textbf{(3.13)}$$

It is shown from the calculations of cooling load for cooling coils that the air volume flow rate is proportional to the cooling load if the entering and leaving air conditions are kept constant, for both sensible cooling load and latent cooling load. When the cooling load in the room is increased, the volume of leaving air of the AHU needs be increased to keep the room at a constant temperature.

3.3.2 Surface condition of cooling coils

The surface condition of the cooling coils will influence the air side heat transfer rate. The surface condition can be divided into three types:

1) Dry condition

If the coil surface temperature at the air outlet is greater than the dew point of the incoming air, then the surface of the coil is completely dry.

2) Wet condition

If the coil surface temperature at the air inlet is less than the dew point of the incoming air, then the coil is completely wet and dehumidification occurs through the surface of the coil.

3) Partially wet condition

Between the completely dry and completely wet surface of the coil, the coil is under the partially wet condition. There is a dry-wet boundary which divides the coil between the dry and wet surface.

For the dry condition, the cooling process only includes the sensible cooling process, and the humidity ratio *w* is always constant. It can be indicated by a horizontal line toward the saturation curve on the psychrometric chart.

However, for most cooling processes in the cooling coil, the dew point temperature of the entering air is higher than the cooling coil surface temperature, so it will be under wet or partially wet conditions. For these conditions, water vapor in the entering air will be condensed and then the condensate will be drained out. The cooling coil will not only cool the air, but also dehumidify the air. The cooling and dehumidifying process can be shown in the psychrometric chart in Figure 3.5. For the partially wet condition, the cooling coil surfaces carry both latent heat and sensible heat.

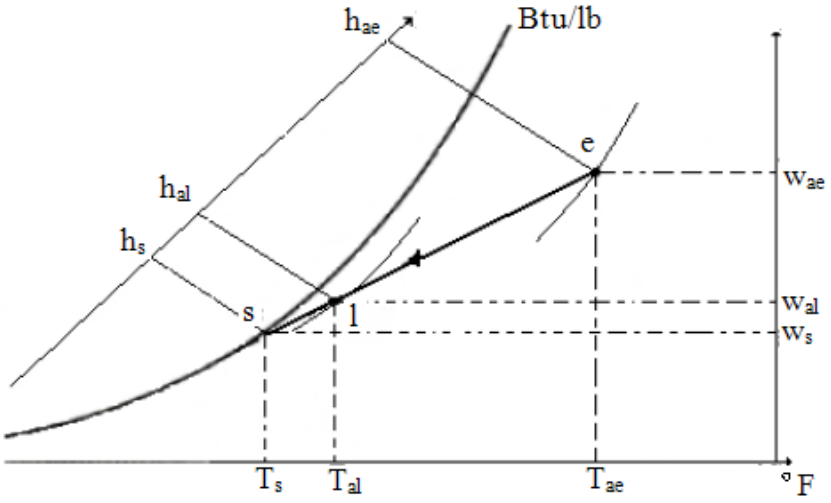

Figure 3.5 Psychrometric chart of cooling and dehumidifying process (Bourabaa et al., 2011)

3.3.3 Air side heat transfer model

The air side performance of plain-finned tube heat exchangers under dehumidifying conditions is calculated by the following model derived from Wang et al. (2000):

$$h = \frac{jG_{max}C_p}{Pr^{\frac{2}{3}}} \tag{3.14}$$

$$j = 19.36\, Re_D^{j_1} \left(\frac{\delta_F}{D}\right)^{1.352} \left(\frac{X_l}{X_t}\right)^{0.6795} N^{-1.291} \tag{3.15}$$

$$j_1 = 0.3745 - 1.554 \left(\frac{\delta_F}{D}\right)^{0.24} \left(\frac{X_l}{X_t}\right)^{0.12} N^{-0.19} \tag{3.16}$$

G_{max}— maximum mass flux of the air

δ_F— fin pitch, ft

D— outside diameter of the tube, ft

X_l— longitude tube pitch, ft

X_t— transverse tube pitch, ft

N— the number of fins per inch

The method to calculate the air side heat transfer coefficient of plain-finned tube heat exchangers under dry surface conditions is as follows, which is proposed by Wang et al. (1996):

$$h = \frac{jG_{max}C_p}{Pr^{\frac{2}{3}}} \quad \textbf{(3.17)}$$

$$j = 0.394Re_D^{-0.392}\left(\frac{\delta_F}{D}\right)^{-0.0449}\left(\frac{F_p}{D}\right)^{-0.212} \quad \textbf{(3.18)}$$

Figure 3.6 and Figure 3.7 show the air side heat transfer coefficient versus air Reynolds number and air velocity. The air conditions simulated in the figures are as follows: (1) the entering air temperature DB/WB temperature: 82/68 ˚F; (2) the leaving air DB/WB temperature 55/55 ˚F, and (3) the average air temperature DB/WB temperature: 68/62 ˚F.

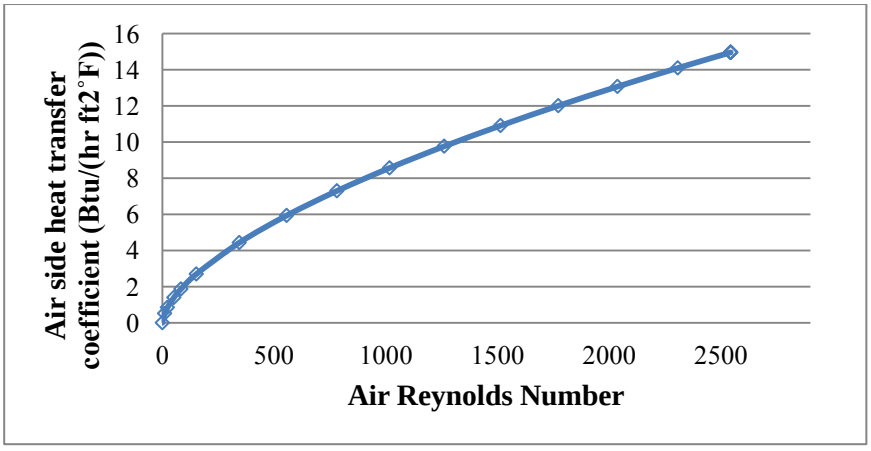

Figure 3.6 Air side heat transfer coefficient vs. air Reynolds number

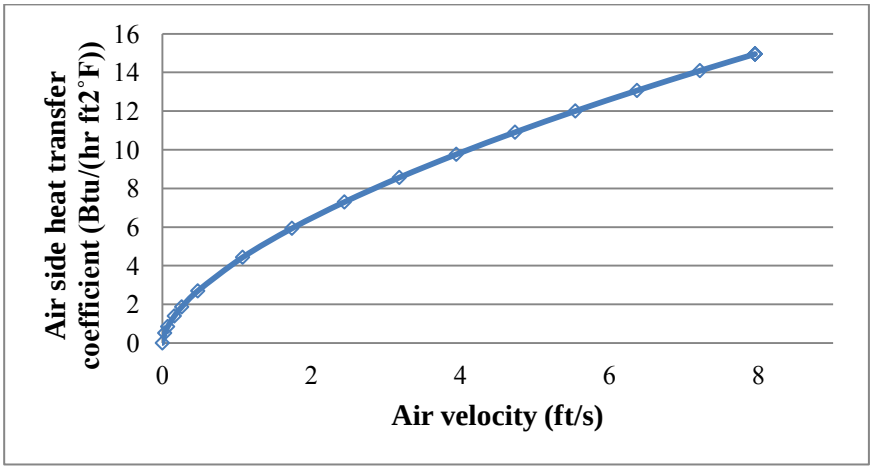

Figure 3.7 Air side heat transfer coefficient vs. air velocity

3.4 Overall heat transfer coefficient of cooling coil

The overall heat transfer coefficient for a heat exchanger can be calculated if the water side and air side heat transfer coefficients are known:

$$\frac{1}{UA_a} = \frac{1}{\eta h_a A_a} + \frac{dx_w}{kA_w} + \frac{1}{h_w A_w} \qquad \textbf{(3.19)}$$

Where η is the total efficiency of the air side surface, which is assumed to be 0.85 in this case; k is the thermal conductivity of the tube wall. The thermal resistance of the tube wall is negligible, so the overall heat transfer coefficient for the heat exchanger can be simplified to:

$$\frac{1}{UA_a} = \frac{1}{\eta h_a A_a} + \frac{1}{h_w A_w} \qquad \textbf{(3.20)}$$

So

$$UA_a = \frac{\eta h_a A_a \times h_w A_w}{\eta h_a A_a + h_w A_w} \qquad \textbf{(3.21)}$$

Figure 3.8 shows that the overall heat transfer coefficient decreases as the water Reynolds number decreases. When the water flow becomes laminar flow and the air velocity becomes constant due to the minimum air flow rate setpoint for the SDVAV system, since the water side heat transfer coefficient keeps uniform as well as the air side heat transfer coefficient, the overall heat transfer coefficient is constant. According to the change of the overall heat transfer coefficient, the heat transfer performance is better for the water flow under the turbulent regime.

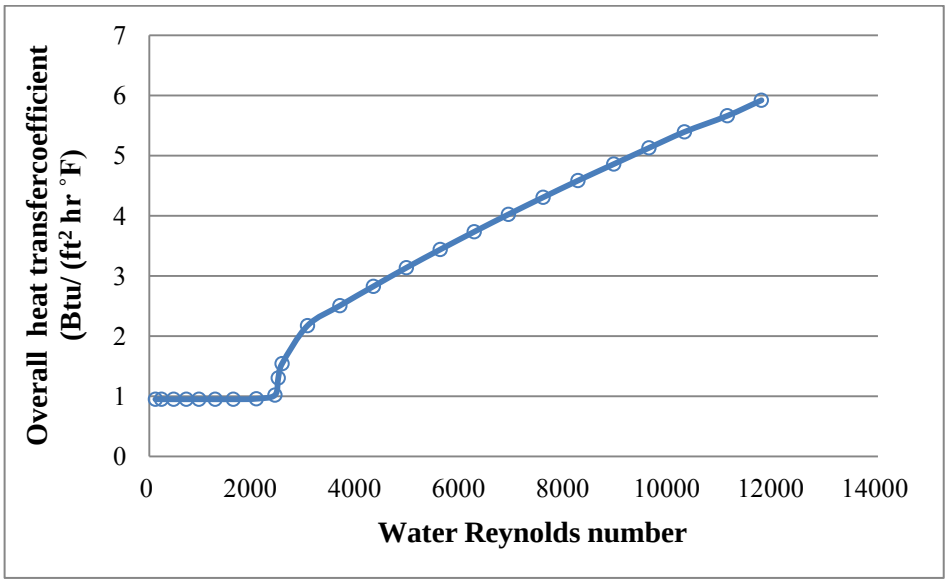

Figure 3.8 Overall heat transfer coefficient vs. water Reynolds number

3.5 Cooling coil effectiveness calculation method

The effectiveness-NTU model proposed by Braun (1989) is used to model the heat transfer performance in the cooling coils. The calculation of the heat transfer rate is based on the concept of an efficiency rating and is defined by the following equation:

$$\varepsilon = \frac{\dot{Q}}{\dot{Q}_{max}} \tag{3.22}$$

The Ntu is broken up into the outside parts and inside parts:

$$NTU_o = \frac{h_o A_o}{\dot{m}_a c_{pa}} \tag{3.23}$$

$$NTU_i = \frac{h_i A_i}{\dot{m}_w c_{pw}} \tag{3.24}$$

3.5.1 Dry conditions

If the surface of the cooling coil is dry, the heat transfer can be described in the following way:

$$\dot{Q}_{dry} = \varepsilon_{dry} \dot{m}_a c_{pa} (T_{ae} - T_{we}) \tag{3.25}$$

$$C_a = \dot{m}_a c_{pa} \tag{3.26}$$

$$C_w = \dot{m}_w c_{pw} \tag{3.27}$$

$$C_{min} = \min (C_a, C_w) \tag{3.28}$$

$$C_{max} = \max (C_a, C_w) \tag{3.29}$$

$$C = \frac{C_{min}}{C_{max}} \tag{3.30}$$

In this case, $C_{min} = C_a$, C_{max}=C_w

Assume:

$$C = \frac{C_a}{C_w} = \frac{\dot{m}_a c_{pa}}{\dot{m}_w c_{pw}} \tag{3.31}$$

The overall number of transfer units for the dry coil is:

$$Ntu_{dry} = \frac{Ntu_o}{1 + C \times \frac{Ntu_o}{Ntu_i}} = \frac{U_o A_o}{\dot{m}_a c_{pa}} \quad \textbf{(3.32)}$$

Effectiveness (ε) varies for different flow patterns. Since the cooling coil is the combination of cross-flow and counter-flow, and ε for these two flow patterns are very close, the efficiency calculation method used here is for the counter-flow correlation:

$$\varepsilon_{dry} = \frac{1 - exp(-Ntu_{dry} \times (1 - C))}{1 - C \times exp(-Ntu_{dry} \times (1 - C))} \quad \textbf{(3.33)}$$

3.5.2 Wet conditions

If the surface of the cooling coil is wet, the enthalpy change of the air will be considered in order to calculate the heat transfer in the coil:

$$\dot{Q}_{wet} = \varepsilon_{wet} \dot{m}_a (h_{ae} - h_{s,we}) \quad \textbf{(3.34)}$$

The average saturation specific heat (C_s), is defined as the average slope between the entering and leaving water conditions:

$$C_s = \frac{h_{s,we} - h_{s,wl}}{T_{we} - T_{wl}} \quad \textbf{(3.35)}$$

Assume:

$$m^* = \frac{\dot{m}_a C_s}{\dot{m}_w c_{pw}} \quad \textbf{(3.36)}$$

The overall number of transfer units for the wet coil is:

$$Ntu_{wet} = \frac{Ntu_o}{1 + m^* \times \frac{Ntu_o}{Ntu_i}} \quad \textbf{(3.37)}$$

Similar to the effectiveness of the dry coil, the effectiveness of the wet coil can be obtained from the following equation:

$$\varepsilon_{wet} = \frac{1 - exp(-Ntu_{wet} \times (1 - m^*))}{1 - m^* \times exp(-Ntu_{wet} \times (1 - m^*))} \quad \textbf{(3.38)}$$

3.5.3 Partially wet conditions

For the partially wet condition, Braun (1989) proved that both completely dry and completely wet analyses underpredict the heat transfer for the cooling coil under the partially wet condition. However, the difference between the heat transfer value for the dry/wet condition and the partially wet condition is generally less than 5%. As a result, Braun (1989) proposed a simple approach to determine the heat transfer for a coil under a partially wet condition: choose the model of a dry or a wet surface condition which yields the larger heat transfer as the model of the partially wet condition.

In this thesis, the coil surface is completely wet, so the model development follows the effectiveness-NTU method under the wet condition.

3.6 Cooling coil delta-T

The delta-T is an important factor, which shows the heat transfer performance of the cooling coil. If the delta-T in the cooling coil is lower than the design value, the loop delta-T will be affected. Low-loop delta-T in a chilled water system results in low chiller efficiency.

The simulation for the cooling coil delta-T is based on the analysis of a SDVAV system using the cooling coil manufactured by Metrol, so the air volume flow rate changes with the water flow rate proportionally. The design condition of the cooling coil is as follows: entering air DB/WB temperature: 82/68 ˚F, leaving air DB/WB

temperature: 55 ˚F, designed water flow rate: 83 GPM, design air volume flow rate: 21,000 cfm, minimum air volume flow rate: 4,200 cfm (20% of the design air volume flow rate). The chilled water inlet temperature keeps constant in the simulation. The entering air and leaving air temperatures are also constant when the air volume flow rate is larger than the minimum air volume flow rate. When the air volume flow rate decreases to the value smaller than the minimum air volume flow rate (20% of the design air volume flow rate), the inlet temperature is changed to decrease the cooling load.

The procedures to calculate the cooling coil delta-T under design condition is as follows:

(1) Calculate the water heat transfer coefficient.

(2) Calculate the outside air NTU based on $NTU_o = \frac{h_o A_o}{\dot{m}_a c_{pa}}$

(3) Calculate the air heat transfer coefficient.

(4) Calculate the inside water NTU based on $NTU_i = \frac{h_i A_i}{\dot{m}_w c_{pw}}$

(5) Determine the dry/wet condition of the cooling coil surface. The surface is wet under the design condition, so the average saturation specific heat (C_s) can be from the entering and leaving water temperatures: $C_s = \frac{h_{s,we} - h_{s,wl}}{T_{we} - T_{wl}}$.

(6) Assume $m^* = \frac{\dot{m}_a C_s}{\dot{m}_w c_{pw}}$ and the overall NTU for the coil is $Ntu_{wet} = \frac{Ntu_o}{1 + m^* \times \frac{Ntu_o}{Ntu_i}}$.

(7) The effectiveness of the cooling coil is $\varepsilon = \frac{1 - exp(-Ntu_{wet} \times (1 - m^*))}{1 - m^* \times exp(-Ntu_{wet} \times (1 - m^*))}$.

(8) Since the entering air temperature and entering water temperature under the design condition is fixed. The maximum heat transfer rate can be obtained from $Q_{max} = \dot{m}_a c_{pa}(T_{ae-}T_{we})$.

(9) The actual heat transfer rate can be calculated from $Q_{act} = \varepsilon \times Q_{max}$.

(10) The cooling coil chilled water can be derived from *delta-T* $= \frac{Q_{act}}{500 \times \text{GPM}}$

The calculations for the cooling coil delta-T at partial loads conditions is similar to the procedures above.

Although the heat transfer rate drops when the air volume flow rate and water flow rate is decreased, the effectiveness of the cooling coil increases with the rise of the water flow rate (see Figure 3.9). The chilled water delta-T in the cooling coil is related to both the heat transfer rate and the effectiveness of the coil.

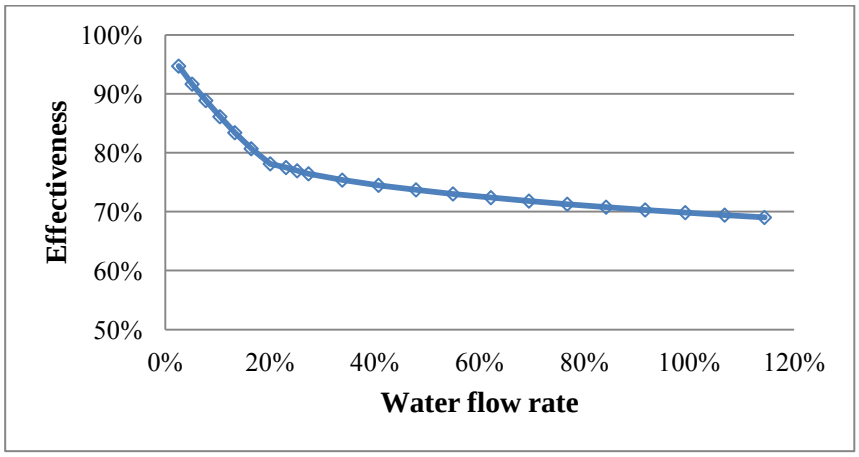

Figure 3.9 Cooling coil effectiveness under different water flow rates

Based on the effectiveness-NTU model, the delta-T of the cooling coil can be obtained. Figure 3.10 shows that the delta-T changes with the total cooling load. When the water in the tubes is under a turbulent flow condition, the delta-T can be taken as constant. However, transitional flow happens when the cooling load and the water flow rate decrease; the delta-T drops significantly. Contrary to the opinion that the cooling coil delta-T will continue to decrease in the laminar flow region, the delta-T increases when the water flow rate becomes lower and the flow condition becomes laminar.

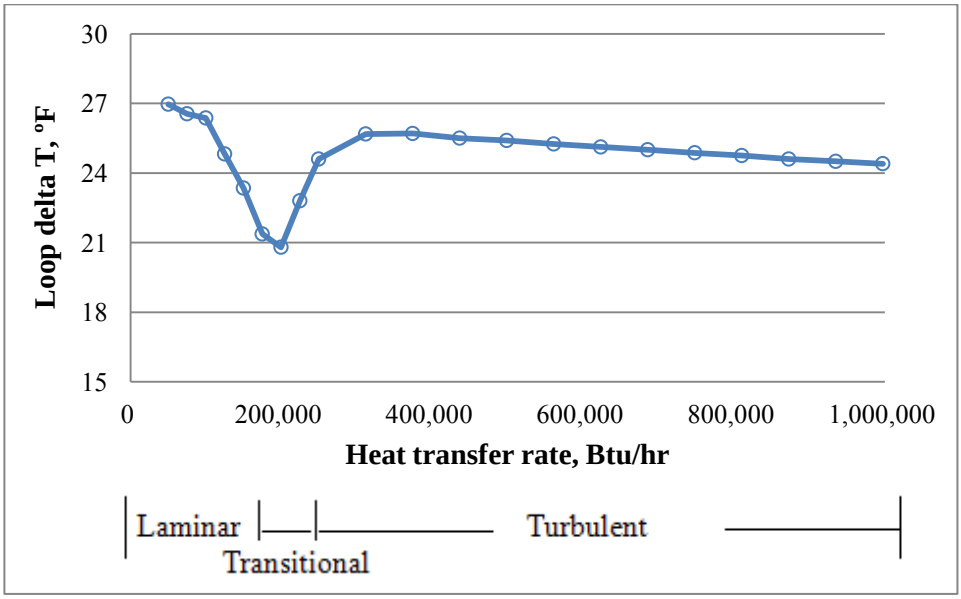

Figure 3.10 Cooling coil delta-T under various cooling loads

4 APPLICATIONS

4.1 System introduction

4.1.1 System configuration

The system studied in this thesis is the chilled water system in the DFW Airport. Due to the change of outside air temperature and the number of passengers in the terminals, the cooling load of the chilled water system changes throughout the year. The low delta-T syndrome exists in the chilled water system under low cooling loads. The objective of this thesis is to analyze the possible causes for the low delta-T syndrome for the chilled water system in the DFW Airport. The main utility tunnel in the DFW Airport houses the main chilled water loop with 36-inch supply and return pipes, which serve the Terminals A through E and various airport buildings. The CUP chilled water system contains six 5,500 ton on-site manufactured (OM) chillers, a 90,000 ton-hr Thermal Energy Storage (TES) tank, six 150 hp constant-speed primary pumps, and four 450 hp variable-speed secondary pumps. The current schematic diagram of the chilled water system in the DFW Airport is shown in Figure 4.1.

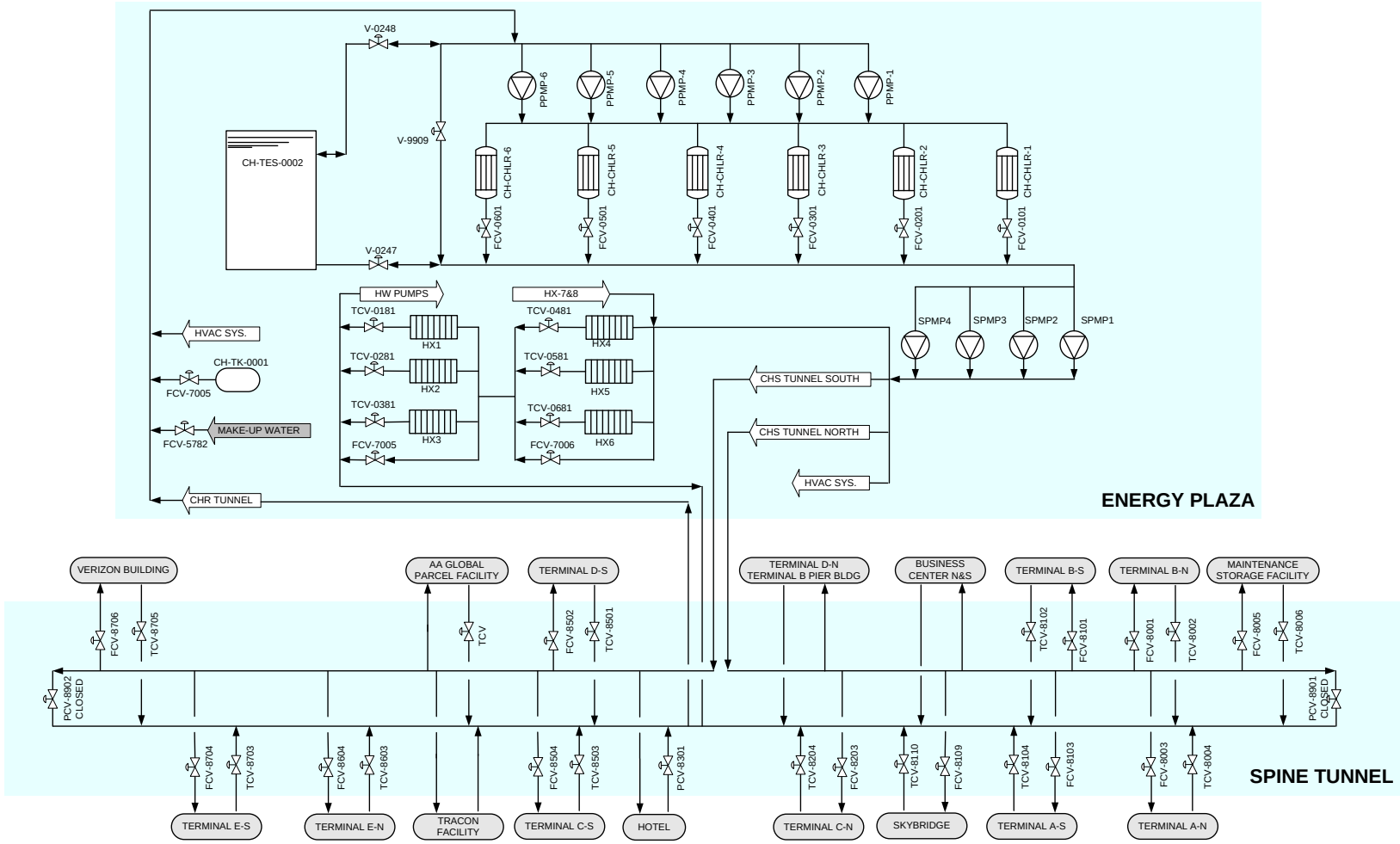

Figure 4.1 Schematic diagram of the CHW system in the DFW Airport (ESL, 2011)

4.1.2 Loop delta-T

There are five terminals in the DFW Airport, which take about 90% chilled water flow in the chilled water system. Each terminal is divided into two loops: a north loop and a south loop. Each loop has its own chilled water supply pipelines. Although the cooling loads and chilled water flow rates in the ten loops are different, due to the difference in occupancy and equipment, they have similar chilled water system configurations and chilled water flow patterns. Terminal B South and Terminal D North are taken as the two examples for the study of the characteristics of the chilled water system. The scatter plots in Figure 4.2 and Figure 4.3 show the chilled water loop delta-T in Terminal B South and Terminal D North under different total cooling loads based on the measured data in 2010.

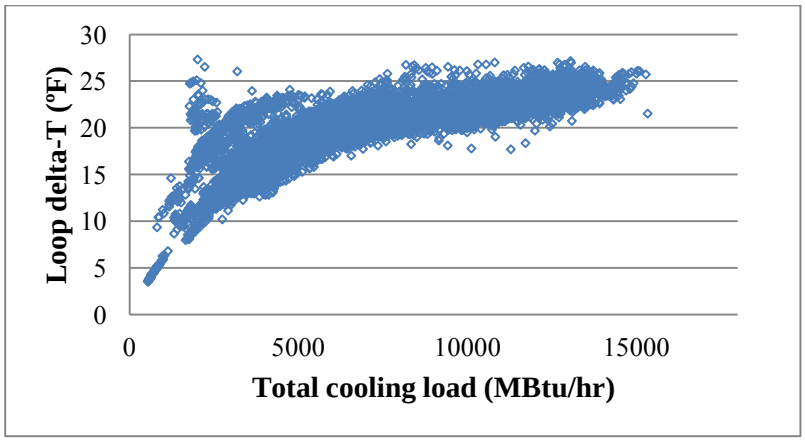

Figure 4.2 Loop delta-T vs. cooling load for Terminal B South

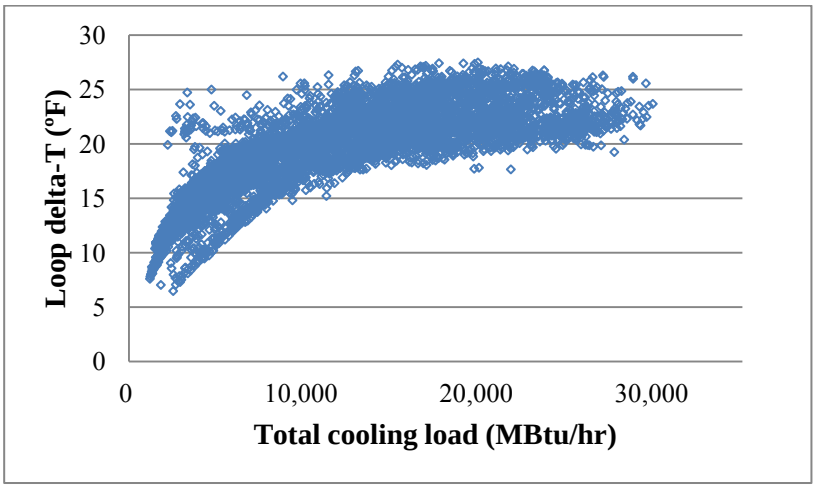

Figure 4.3 Loop delta-T vs. cooling load for Terminal D North

The maximum cooling load for Terminal D North throughout the year is about 30,000 MBtu/hr and the minimum cooling load is about 1,500 MBtu/hr. The loop delta-T is stable and can be taken as constant when the cooling load is higher than 10,000 MBtu/hr, which is about 30% of the maximum load. The delta-T falls dramatically when the cooling load decreases and the load is lower than 10,000 MBtu/hr. This phenomenon also exists in Terminal B South and other terminals, especially under the low cooling load conditions.

According to the measured data for Terminal D North in the DFW Airport, the loop delta-T throughout 2010 is shown in Figure 4.4, the loop delta-T in the winter is about 15 ºF, which is much lower than that in the summer.

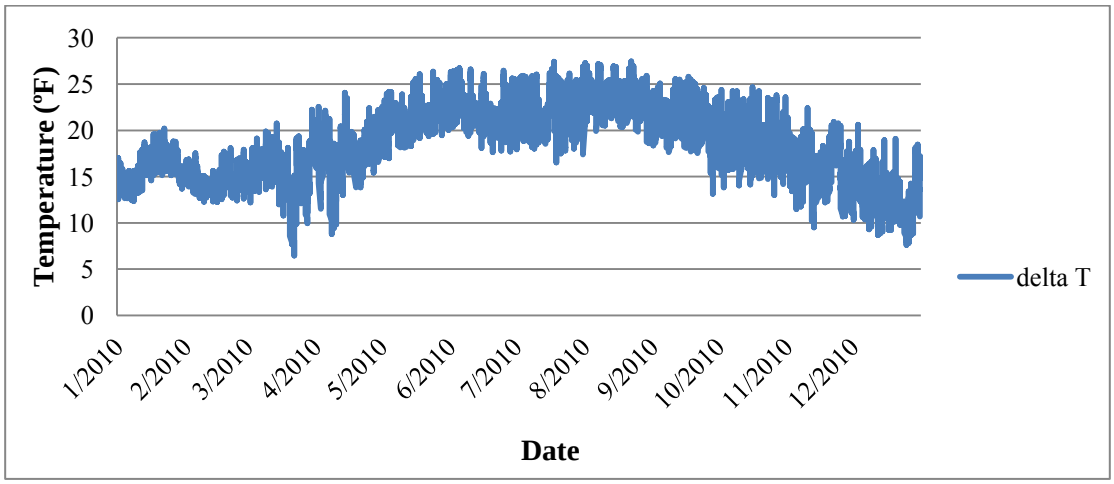

Figure 4.4 Loop delta-T of the Terminal D North in the DFW Airport for 2010

The scatter plots of the loop delta-T for Terminal B South and Terminal D North under different total cooling loads and supply chilled water temperatures are shown in Figure 4.5 and Figure 4.6. These figures show that when the chilled water supply temperature is lower than 39 ˚F, the difference between the low delta-T and high delta-T under the same cooling load is larger than the case under the higher supply chilled water temperature. Moreover, the system delta-T under low supply chilled water temperature also appears to be lower than the delta-T under higher supply chilled water temperature.

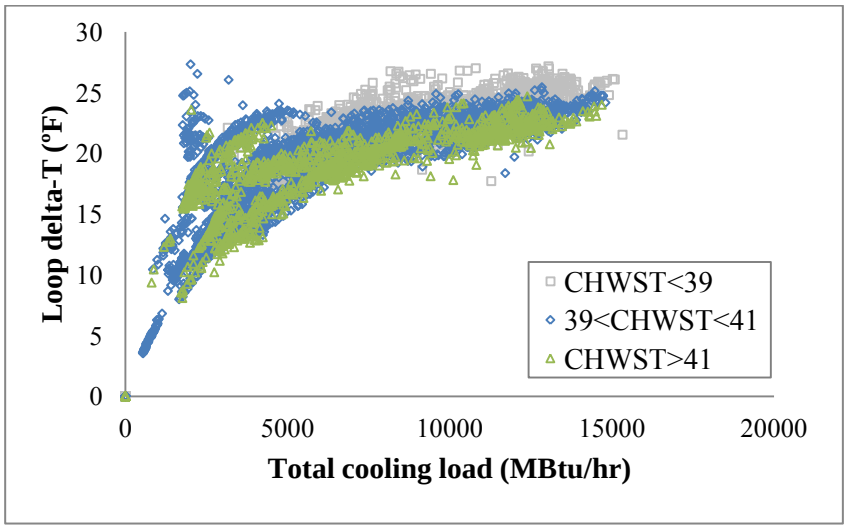

Figure 4.5 Loop delta-T under different cooling loads and chilled water supply temperatures for Terminal B South

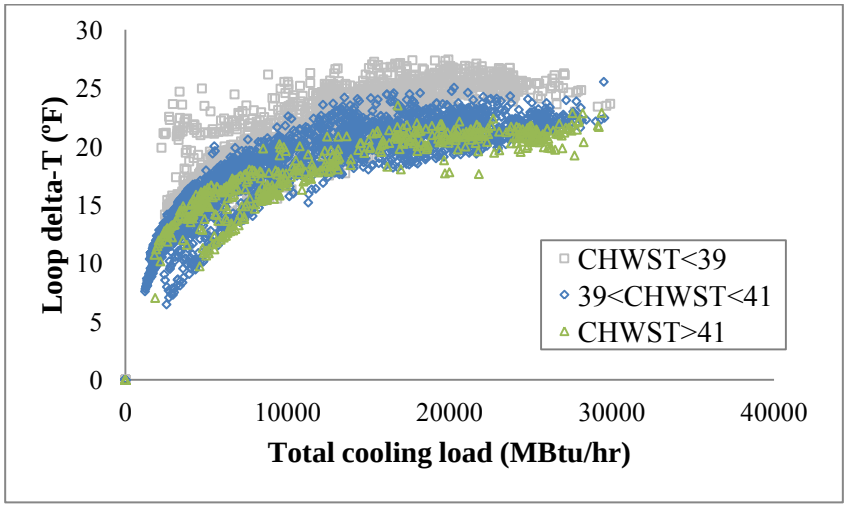

Figure 4.6 Loop delta-T under different cooling loads and chilled water supply temperatures for Terminal D North

4.2 Laminar flow in the cooling coils

Although the cooling coil delta-T in the DFW Airport will drop when the water flow enters the transitional flow and laminar flow region, delta-T in the laminar flow region should increase according to the results of this thesis. The largest delta-T difference in the turbulent region and the transitional/laminar region is about 6 ºF for the cooling coil studied in this thesis, and it is only 3 ºF below the design delta-T (24 ºF). However, delta-T in the loop of the DFW Airport under low load conditions reaches as high as 10 ºF comparing with the setpoint of the delta-T. As a result, the cooling coil performance in the laminar flow regime should not be the main reason for the degradation of chilled water delta-T at low loads. Consequently, other factors may exist in the current system which lead to the low delta-T syndrome at low water flow rates. The following part of this section will further discuss possible piping strategy causes for the low delta-T syndrome of the chilled water system in the DFW Airport.

4.3 Piping strategy

4.3.1 Use of three-way valves

Valves are used to control the flow of water through a coil in order to vary the heat transfer rate in chilled water systems. In large systems, three-way valves are sometimes installed at the terminal end (Figure 4.7). Three-way valves bypass unheated chilled water around the cooling coil then into the return line. This approach keeps water constantly moving through the circuit so that chilled water will be available immediately on demand by any coil in the system. However, the systems with three-way valves

operate with constant flow, which is detrimental to the system delta-T. The disadvantages for the use of three-way valve is also demonstrated by Fiorino (1999).

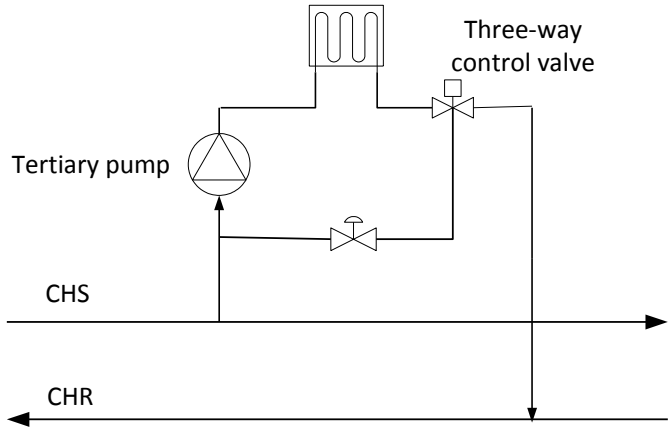

Figure 4.7 Chilled water loop with three-way valve

As shown in Figure 4.8, for an AHU with a three-way valve, the chilled water return temperature from the AHU is always lower than that from the coil for partial load conditions. The design chilled water supply temperature is 38 ˚F and the design chilled water return temperature is 62 ˚F. The chilled water return temperature is directly correlated with the size of the load. As a result, lower chilled water return temperatures are associated with smaller loads in the system with a three-way valve. For a system with a two-way valve, the chilled water return temperatures from the coil and AHU are the same. Consequently, a low delta-T syndrome in the system can be avoided. It is seen that using three-way valves in a system may result in a low delta-T syndrome. In addition, three-way valves increase pump and chiller energy consumption. It is strongly suggested that three-way valves should not be used in variable flow systems.

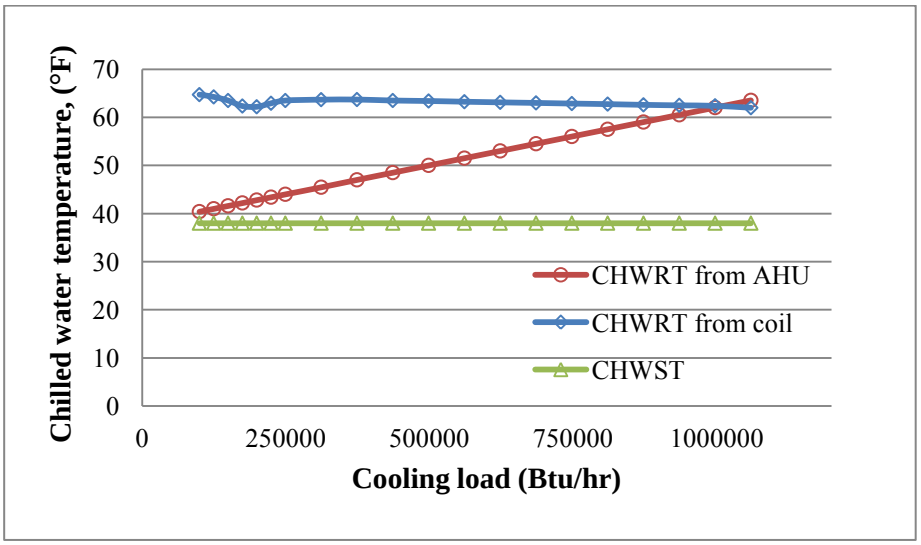

Figure 4.8 Chilled water temperature in the system with three-way control valve

4.3.2 Use of two-way valves

Considering that the use of three-way valves may lead to the low delta-T syndrome, two-way control valves should be used in the chilled water loops.

To reduce the pump energy consumption, the DFW Airport plans to add tertiary pumps to the terminals and buildings along the main loop of the chilled water system (ESL, 2011). Meanwhile, in order to keep the chilled water delta-T, the installation of two-way valves in the system is suggested. There are three methods to install the tertiary pumps and two-way valves:

1. Tertiary pumping schematic 1: without a two-way valve (Figure 4.9). This method is used to assist where the pressure drop for a specific load is greater than the pressure differential available in the main secondary loop. This condition often occurs

when a new load is added to an existing loop. The tertiary pump is added to provide additional pressure to overcome the specific load.

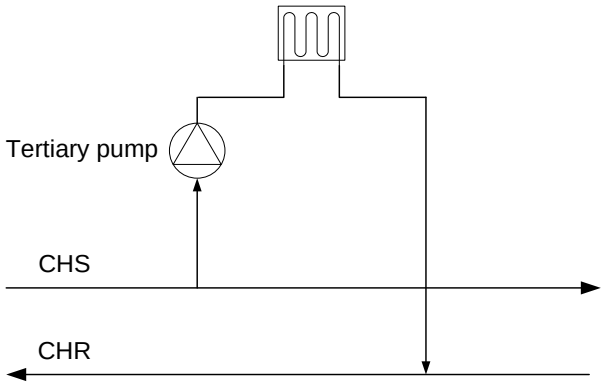

Figure 4.9 Tertiary pumping schematic 1

2. Tertiary pumping schematic 2: with a two-way control valve and bypass line (Figure 4.10). The method provides the necessary flow and head for the loop it serves. If the two-way valve is closed, the chilled water recirculates through the common pipe. If the valve is opened, water is returned while cooling chilled water is introduced. The design chilled water temperature in the tertiary loop must be warmer than the main supply chilled water temperature. If they are the same temperature, the two-way control valve will open and bleed supply water into the return line leading to a low delta T syndrome. The tertiary pumping method with a two-way control value is usually effective in a system where a load requires a different temperature range than the main system.

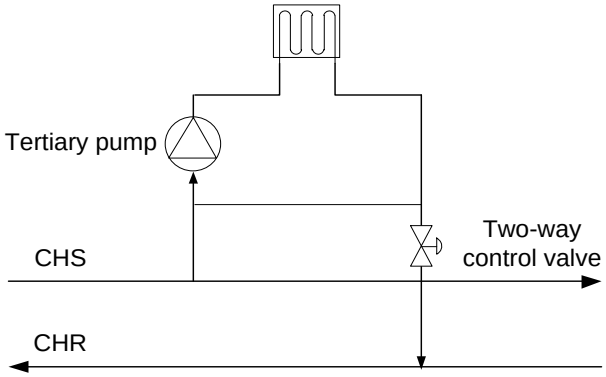

Figure 4.10 Tertiary pumping schematic 2

3. Tertiary pumping schematic 3: with a two-way control valve and check valve in the bypass line (Figure 4.11). This method ensures that the chilled water supply will never be bypassed through the common leg to the return by using the check valve. As a result, loop water flow will always equal or exceed that supplied from the secondary system (Avery, 1998).

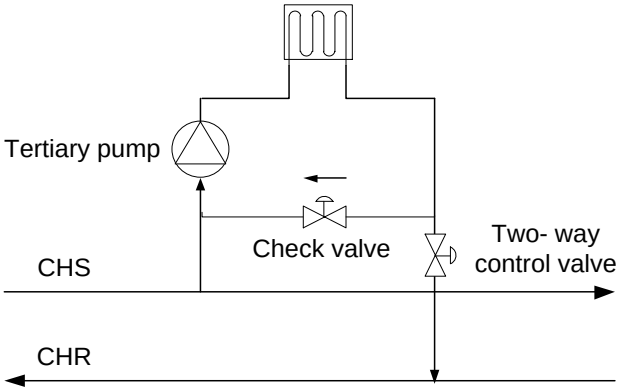

Figure 4.11 Tertiary pumping schematic 3

5 SUMMARY

The cooling coil is an important part in chilled water systems. When the cooling load is low and water flow rate decreases to a certain level in the cooling coil, laminar flow occurs in the tubes. As a result, both the water side and air side heat transfer coefficients will decrease and lead to the sudden drop of the overall heat transfer coefficient of the cooling coil, which will have a negative influence for the heat transfer performance. However, when the air velocity decreases, the coil effectiveness will increase, which compensates for the drop of the overall heat transfer coefficient.

This thesis studied the cooling coil that will be installed in the DFW Airport. The performance study is based on the effective-NTU method proposed by Braun (1989). The results for the delta-T of the cooling coil under different load conditions shows that the chilled water delta-T decreases after the water flow rate decreases and that the flow becomes transitional flow. However, delta-T increases in the laminar flow regime due to the rise of the coil effectiveness in this regime. The largest drop for the delta-T in the cooling coil from the low water flow rate is about 5 ºF and only 3 ºF below the design temperature difference, which does not have a significant effect on the delta-T of the chilled water system.

From the above discussions, it can be concluded that laminar flow in the cooling coil is not the major cause for the low delta-T syndrome in the chilled water systems. However, based on the 2010 data of the chilled water system in the DFW Airport, the low delta-T can be found when the cooling load is lower than 30% of the maximum

cooling load, and the drop of delta-T can even reach 50%. Some other factors may exist in the system and influence the system performance.

The piping strategy may affect the system delta-T. The three-way control valves bypass part of the chilled water instead of routing it through the cooling coils, so the use of three-way valves will increase the chilled water return temperature. There are three methods by which two-way valves may avoid low delta-T syndrome in the loops: (1) without a two-way valve; (2) with a two-way valve and a bypass line; and (3) with a two-way valve and a check valve in the bypass line, to implement the tertiary pumps and two-way valves for different needs in the chilled water system. Improper tertiary pump installation strategy will also have negative influence for the chilled water delta-T.

In conclusion, the low delta-T syndrome in the DFW Airport is not primarily due to laminar flow under low-load conditions. In order to optimize the existing low delta-T syndrome in the DFW airport, more measures should be considered in the chilled water system, such as the use of valves and piping configurations.

6 FUTURE WORK

The simulation in this thesis was performed under the air condition as follows: (1) the entering air temperature DB/WB temperature was 82/68 ˚F; and (2) the leaving air DB/WB temperature was 55/55 ˚F. The entering air temperature is chosen based on the design condition of the cooling coil, but may vary when the outside air temperature changes. The entering air temperature will decrease when the outside air temperature decreases, and it will also have influence on the dry or wet condition of the cooling coil surface. Expanded studies for the cooling coil performance under different entering air conditions will be valuable to evaluate the cooling coil operation more completely.

More measurement and analysis should be taken for the chilled water system in the DFW Airport. Possible causes rather than the cooling coil performance under low cooling loads and improper piping strategy may also lead to the low delta-T in the system. The scatter plots of the loop delta-T for Terminal B South and Terminal D North under different total cooling loads and supply chilled water temperatures are shown in Figure 4.5 and Figure 4.6. They show that when the chilled water supply temperature is lower than 39 ˚F, the difference between the low delta-T and high delta-T under the same cooling load is larger than the case under the higher supply chilled water temperature, and the system delta-T under low supply chilled water temperature also appears to be lower than the delta-T under higher supply chilled water temperature. More studies which can help to verify the influence of the chilled water supply

temperature on the chilled water delta-T will also be helpful to improve the efficiency and optimize the operation of the chilled water .

REFERENCES

ASHRAE. 2004. *ASHRAE Handbook: HVAC Systems and Equipment*. American Society of Heating, Refrigerating, and Air-Conditioning Engineers, Atlanta, GA.

ASHRAE. 2005. *ASHRAE Handbook: Fundamentals*. American Society of Heating, Refrigerating, and Air-Conditioning Engineers, Atlanta, GA.

Avery, G. 1998. Controlling chillers in variable flow systems. *ASHRAE Journal* 40(2):42-45.

Bourabaa, A., M. Saighi, and I. Belal. 2011. The influence of the inlet conditions on the air side heat transfer performance of plain finned evaporator. *World Academy of Science, Engineering and Technology* 59(7): 28-31.

Braun, J. E. 1989. Effectiveness models for cooling towers and cooling coil. *ASHRAE Transactions* 96(2): 164-167.

Coad, W. J. 1998. A fundamental perspective on chilled water systems. *HPAC Engineering* 70(8): 59-66.

Dittus, F. W., and L. M. K. Boelter. 1930. Heat transfer in automobile radiators of the tubular type. *University of California Publications of Engineering* 2: 443-461.

Energy Information Administration (EIA). 2010. Annual energy review 2010, *Report* DOE/EIA-0384 (2010). U.S. Department of Energy, Washington, DC.

Energy Systems Laboratory. 2011. Final Report: Dallas/Fort Worth International Airport (DFW) Central Utility Plant Hydraulic Systems Analysis.

Erek, A., Ö. Barış, B. Levent, and İ. Zafer. 2005. Effect of geometrical parameters on heat transfer and pressure drop characteristics of plate fin and tube heat exchangers. *Applied Thermal Engineering* 25(14-15): 2421-2431.

Fiorino, D. P. 1999. Achieving high chilled-water delta-Ts. *ASHRAE Journal* 41(11): 24-30.

Gnielinski, V. 1976. New equations for heat and mass transfer in turbulent pipe and channel flow. *International Chemical Engineering* 16(2): 359-368.

Green Building HVAC. Selection of Cooling Coils to Avoid Low Delta-T Syndrome. Retrieved 04/05, 2012, from http://www.thegreenbuildinghvac.com/?cat=123&paged=2

Hartman T. 2001. Getting real about low delta T in variable-flow distribution systems. *HPAC Engineering* 73(4):17-22.

Incropera, F., and D. DeWitt. 2002. *Fundamentals of Heat and Mass Transfer*. Hoboken: Wiley.

Khan, W. A., J. R. Culham, and M. M. Yovanovich. 2006. Convection heat transfer from tube banks in crossflow: analytical approach. *International Journal of Heat and Mass Transfer* 49(25-26): 4831-4838.

Kirsner, W. 1996. Demise of the primary-secondary pumping paradigm for chilled water plant design. *HPAC Engineering* 68(11): 73-78.

Kirsner, W. 1998. Rectifying the primary-secondary paradigm for chilled water plant design to deal with low ΔT central plant syndrome. *HPAC Engineering* 70(1): 128-131.

Landman. 1991. A new era of free cooling. *Trane Engineers Newsletter* 20(3): 1-7.

Liu, J., J. Wei, G. Ding, C. Zhang, et al. 2004. A general steady state mathematical model for fin-and-tube heat exchanger based on graph theory. *International Journal of Refrigeration* 27(8): 965-973.

Ma, Z., S. Wang, and D. Gao. 2010. Performance enhancement of a complex chilled water system using a check valve: experimental validation. *Applied Thermal Engineering* 30 (17-18): 2827-2832.

McQuiston F.C. 1978. Heat mass and momentum transfer data for five plate-fin-tube heat transfer surfaces. *ASHRAE Transactions* 84(1): 266-293

Mirth, D. R., S. Ramadhyani, and D. C. Hittle. 1993. Thermal performance of chilled-water cooling coils operating at low water velocities. *ASHRAE Transactions* 99(1): 43-53.

Montgomery, R., and R. McDowall. 2009. *Fundamentals of HVAC Control Systems*. American Society of Heating, Refrigerating, and Air-Conditioning Engineers, Atlanta, GA.

Neal C. 2011. Submittal data for Dallas Fort Worth Airport TRIP terminal A SA-05.

Nonnenmann, J. J. Chilled Water Plant Pumping Schemes. Retrieved 06/14, 2012, from http://www.stanford.edu/group/narratives/classes/08-09/CEE215/ReferenceLibrary/Pumps/Chilled%20Water%20Plant%20Pumping%20Schemes.pdf

Petukhov, B. S. 1970. Heat transfer and friction in turbulent pipe flow with variable physical properties. *Advances in Heat Transfer* 6: 503-564.

Rich, D. G. 1973. The effect of fin spacing on the heat transfer and friction performance of multi-row, smooth plate fin tube heat exchangers. *ASHRAE Transactions* 79(2): 137-145.

Romero-Méndez, R., M. Sen, K. T. Yang, and R. McClain. 2000. Effect of fin spacing on convection in a plate fin and tube heat The effect of the number of tube rows on the heat transfer and friction performance of multirow smooth plate fin tube heat exchangers. exchanger. *International Journal of Heat and Mass Transfer* 43(1): 39-51.

Severini, S. C. 2004. Making them work: primary-secondary chilled water systems. *ASHRAE Journal* 46(7): 27-33.

Sieder, E. N., and G. E. Tate. 1936. Heat transfer and pressure drop of liquids in tubes. *Industrial Engineering Chemistry* 28: 1429.

Taylor, S.T. 2002. Degrading chilled water plant delta-T: causes and mitigation. *ASHRAE Transaction* 108(1): 641-653.

Taylor, S.T. 2011. Optimizing design & control of chilled water plants part 3: pipe sizing and optimizing ΔT. *ASHRAE Journal* 53(12):22-34.

USA Coil and Air News Letter. Hot Water/ Chilled Water Coils. Retrieved 04/05, 2012, from http://www.usacoil.com/newsletters/aug.pdf

Wang, C., and K. Chi. 2000. Heat transfer and friction characteristics of plain fin-and-tube heat exchangers, part I: new experimental data. *International Journal of Heat and Mass Transfer* 43(15): 2681-2691.

Wang, C., Y. Hsieh, Y. Lin. 1997. Performance of plate finned tube heat exchangers under dehumidifying conditions. *Heat Transfer* 119:109-117.

Wang, C., Y. Lin, C. Lee. 2000. An airside correlation for plain fin-and-tube heat exchangers in wet conditions. *International Journal of Heat and Mass Transfer* 43(10): 1869-1872.

Wang, G, M. Liu, and D. E. Claridge. 2005. Decoupled Modeling of Chilled Water Cooling Coils Using a Finite Element Method. Proceedings of the Fifth International Conference for Enhanced Building Operations, Pittsburgh, PA.

Wang, G., B. Zheng, et al. 2006. Impacts on building return water temperature in district cooling systems. Proceedings of 2006 International Solar Energy Conference, Denver, CO.

Wang, K. S. 1993. *Handbook of Air Conditioning and Refrigeration*. McGraw-Hill, Inc. New York, NY.

Wang, Y., W. Cai, Y. Soh, et al. 2004. A simplified modeling of cooling coils for control and optimization of HVAC systems. *Energy Conversion and Management* 45(18–19): 2915-2930.

Webb, R. L. 1980. Air-side heat transfer in finned tube heat exchangers. *Heat Transfer Engineering* 1 (3): 33-49.

Zhao, X. 1995. Performance of single-row heat exchanger at low in-tube flow rates. Master Dissertation, Department of Aerospace and Mechanical Engineering, University of Notre Dame.

APPENDIX A WATER SIDE HEAT TRANSFER COEFFICIENT CALCULATION

Table A.1 Water properties table

LFT / EFT	38 / 62 ˚F
Design water flow rate / velocity	83 GPM / 2.97 ft/s
Cp	0.98 Btu/lbm.˚F
k	9.45E-05 Btu/s.ft.˚F
μ	8.52E-04 lbm/ft.s
Pr	8.80

Table A.2 Water side heat transfer coefficient calculation sheet

Water velocity (ft/s)	Water flow rate (Gal/min)	Re_w	Nu_w	h_w (Btu/(hr.ft^2.$^\circ$F))
0.019	0.5	65	4.36	40.0
0.033	0.9	116	4.36	40.0
0.066	1.8	231	4.36	40.0
0.132	3.7	463	4.36	40.0
0.20	5.5	698	4.36	40.0
0.27	7.5	939	4.36	40.0
0.34	9.5	1195	4.36	40.0
0.42	11.7	1476	4.36	40.0
0.51	14.3	1803	4.36	40.0
0.59	16.5	2074	4.36	40.0
0.65	18.0	2265	4.36	40.0
0.70	19.6	2460	NA	52.0
0.87	24.2	3039	33.6	76.4
1.04	29.1	3661	38.9	276.51
1.23	34.2	4305	44.3	314.76
1.41	39.3	4940	49.5	351.35
1.59	44.4	5590	54.6	387.90
1.78	49.6	6243	59.7	423.76
1.97	54.8	6901	64.7	459.09
2.16	60.1	7567	69.6	494.24
2.35	65.5	8238	74.5	528.97
2.54	70.9	8925	79.4	564.01
2.73	76.3	9602	84.2	597.96
2.93	81.7	10284	89.0	631.71
3.16	88.3	11109	94.6	671.93
3.35	93.5	11762	99.1	703.37
3.54	98.7	12416	103.5	734.46
3.72	103.9	13069	107.8	765.22

APPENDIX B AIR SIDE HEAT TRANSFER COEFFICIENT CALCULATION

Table B.1 Air properties table

EDB / EWB	82 / 68 ˚F
LDB / LWB	55 / 55 ˚F
Design air volume flow rate	21,000 cfm
Minimum air volume flow rate	4,200 cfm (20% of the design value)
Cp	0.24 Btu/lbm.˚F
k	4.18E-06 Btu/s.ft.˚F
μ	1.24E-05 lbm/ft.s
Pr	0.71

Table B.2 Air side heat transfer coefficient calculation sheet

Air velocity (ft/s)	**Air volume flow rate (cfm)**	**Ga,max (lbm/(ft^2.s))**	**j**	**Re**	**h (Btu/(hr.ft2. ºF))**
1.59	4200	0.120	0.0141	509	1.82
1.62	4273	0.122	0.0140	517	1.84
1.85	4884	0.139	0.0136	591	2.04
2.08	5494	0.156	0.0132	665	2.24
2.31	6105	0.174	0.0129	739	2.43
2.89	7631	0.217	0.0123	924	2.89
3.47	9157	0.261	0.0118	1109	3.33
4.05	10683	0.304	0.0114	1294	3.75
4.62	12209	0.348	0.0111	1478	4.16
5.20	13735	0.391	0.0108	1663	4.55
5.78	15262	0.434	0.0105	1848	4.94
6.36	16788	0.478	0.0103	2033	5.32
6.94	18314	0.521	0.0101	2218	5.69
7.52	19840	0.565	0.0099	2402	6.05
8.09	21366	0.608	0.0097	2587	6.41
8.67	22892	0.652	0.0096	2772	6.76
9.25	24419	0.695	0.0095	2957	7.11
9.83	25945	0.738	0.0093	3142	7.45

APPENDIX C COOLING COIL DELTA-T CALCULATION

Table C.1 Cooling coil delta-T calculation sheet (1)

Entering air DB (ºF)	Entering air WB (ºF)	Entering air enthalpy (Btu/lb)	Leaving air dry/wet bulb T (ºF)	Leaving air enthalpy (Btu/lb)	Air flow rate (cfm)	h_{air} (Btu/(hr.ft^2. ºF))	m_aC_{air}
82.0	59.4	25.8	55.0	23.2	4200.0	1.5	4549.4
82.0	61.2	27.1	55.0	23.2	4200.0	1.5	4549.4
82.0	63.1	28.4	55.0	23.2	4200.0	1.5	4549.4
82.0	64.9	29.8	55.0	23.2	4200.0	1.5	4549.4
82.0	66.6	31.1	55.0	23.2	4200.0	1.5	4549.4
82.0	68.0	32.2	55.0	23.2	4273.3	1.6	4628.7
82.0	68.0	32.2	55.0	23.2	4883.7	1.7	5290.0
82.0	68.0	32.2	55.0	23.2	5494.2	1.9	5951.2
82.0	68.0	32.2	55.0	23.2	6104.7	2.1	6612.5
82.0	68.0	32.2	55.0	23.2	7630.8	2.5	8265.6
82.0	68.0	32.2	55.0	23.2	9157.0	2.8	9918.7
82.0	68.0	32.2	55.0	23.2	10683.1	3.2	11571.9
82.0	68.0	32.2	55.0	23.2	12209.3	3.5	13225.0
82.0	68.0	32.2	55.0	23.2	13735.5	3.9	14878.1
82.0	68.0	32.2	55.0	23.2	15261.6	4.2	16531.2
82.0	68.0	32.2	55.0	23.2	16787.8	4.5	18184.3
82.0	68.0	32.2	55.0	23.2	18314.0	4.8	19837.5
82.0	68.0	32.2	55.0	23.2	19840.1	5.1	21490.6
82.0	68.0	32.2	55.0	23.2	21366.3	5.4	23143.7

Table C.2 Cooling coil delta-T calculation sheet (2)

Entering Water temperature (°F)	Water flow rate (fpm)	h_{water} (Btu/(hr.ft^2. °F))	m_wC_{water}
38.0	3.7	40.0	1799.0
38.0	5.5	40.0	2710.5
38.0	7.5	40.0	3649.2
38.0	9.5	40.0	4643.1
38.0	11.7	40.0	5735.6
38.0	14.3	40.0	7007.6
38.0	16.5	40.0	8058.3
38.0	18.0	40.0	8800.1
38.0	19.6	52.0	9559.4
38.0	24.2	76.4	11810.3
38.0	29.1	276.5	14227.5
38.0	34.2	314.8	16728.9
38.0	39.3	351.3	19194.0
38.0	44.4	387.9	21721.6
38.0	49.6	423.8	24260.0
38.0	54.8	459.1	26814.1
38.0	60.1	494.2	29404.6
38.0	65.5	529.0	32009.4
38.0	70.9	564.0	34681.9

Table C.3 Cooling coil delta-T calculation sheet (3)

Cs	m*	Ntu wet	Fin effectiveness	Leaving water temperature (ºF)	Cooling coil delta-T (ºF)
0.653	6.9	0.8	92%	65.0	27.0
0.640	4.6	1.1	89%	64.6	26.6
0.635	3.4	1.3	86%	64.4	26.4
0.587	2.6	1.4	83%	62.8	24.8
0.544	2.0	1.4	81%	61.4	23.4
0.487	1.6	1.4	78%	59.4	21.4
0.471	1.6	1.4	77%	58.8	20.8
0.528	1.7	1.6	77%	60.8	22.8
0.581	1.8	1.8	76%	62.6	24.6
0.617	1.8	1.9	75%	63.8	25.7
0.614	1.8	1.8	74%	63.7	25.7
0.608	1.8	1.8	74%	63.5	25.5
0.605	1.7	1.7	73%	63.4	25.4
0.600	1.7	1.7	72%	63.3	25.3
0.596	1.7	1.6	72%	63.1	25.1
0.593	1.7	1.6	71%	63.0	25.0
0.589	1.7	1.6	71%	62.9	24.9
0.585	1.6	1.5	70%	62.8	24.8
0.581	1.6	1.5	70%	62.6	24.6